

Supplementary data - Report 34: COVID-19 Infection Fatality Ratio: Estimates from Seroprevalence

Nicholas F Brazeau¹, Robert Verity¹, Sara Jenks², Han Fu¹, Charles Whittaker¹, Peter Winskill¹, Ilaria Dorigatti¹, Patrick Walker¹, Steven Riley¹, Ricardo P Schnekenberg³, Henrique Hoeltgebaum⁴, Thomas A Mellan¹, Swapnil Mishra¹, H Juliette T Unwin¹, Oliver J Watson¹, Zulma M Cucunubá¹, Marc Baguelin¹, Lilith Whittles¹, Samir Bhatt¹, Azra C Ghani¹, Neil M Ferguson¹, Lucy C Okell¹⁺.

¹ MRC Centre for Global Infectious Disease Analysis & WHO Collaborating Centre for infectious Disease Modelling; Abdul Latif Jameel Institute for Disease and Emergency Analytics (J-IDEA), School of Public Health, Imperial College London, UK

² Department of Clinical Biochemistry, Royal Infirmary of Edinburgh, Edinburgh, UK

³ Nuffield Department of Clinical Neurosciences, University of Oxford

⁴ Department of Mathematics, Imperial College, London, UK

Correspondence: Dr Lucy Okell l.okell@imperial.ac.uk

SUGGESTED CITATION

NF Brazeau, R Verity, S Jenks *et al.* COVID-19 Infection Fatality Ratio: Estimates from Seroprevalence - SUPPLEMENT. Imperial College London (29-10-2020), doi <https://doi.org/10.25561/83545>.



This work is licensed under a Creative Commons Attribution-NonCommercial-NoDerivatives 4.0 International License.

1. Content:

1. Content

2. Data Extraction & Manipulation

2.1.1 Study Screening and Selection for Inclusion

2.1.2 Data Extraction and Collation

2.2 Age-Based Statistical Model Derivation

2.2.1 Daily and age-stratified deaths

2.2.2 Incorporating serology data

2.2.3 Extension for seroreversion

2.2.4 Full model

3. Prior Information and Model Fitting

3.1 Symptom Onset to Seroreversion Parameter Estimation

3.2 Onset-Outcome Delay Distributions and Serological Test Characteristics

3.3 Estimating Specificity: Region-based Statistical Model Description

4. Insights from Simulated Data

5. Age-Based Statistical Model Posteriors

5.1 Posterior Parameter Estimates

5.2 Posterior Predictive Checks

6. Estimating Specificity: Region-based Statistical Model Posteriors

6.1 Posterior Parameter Estimates

7. Pooled IFR Calculation

8. References

2. Data Extraction & Manipulation

2.1.1 Study Screening and Selection for Inclusion

Identification of relevant serological studies was carried out using the `SeroTracker` dashboard ¹, an ongoing and continuously updated systematic review. From `SeroTracker`, a total of 175 severe acute respiratory syndrome coronavirus 2 (SARS-CoV-2) serological studies were screened according to a predefined set of inclusion and exclusion criteria, the details of which are described further in **Supplementary Table 1**.

After screening the studies available on SeroTracker, 10/175 were selected for inclusion. Further information and details of these studies can be found in **Supplementary Table 2**. Excluded studies and the specific reason for exclusion are included as **Additional File 1**.

Supplementary Table 1 - Inclusion and Exclusion Criteria for Seroprevalence Studies: We assumed that dexamethasone treatment was considered routine clinical practice approximately one-month after the RECOVERY trial results were released (*; PMID: 32678530). Studies conducted after the introduction of dexamethasone were excluded, as we assumed that this change in clinical practice caused shifts in the IFR that were not comparable to pre-treatment periods.

Inclusion Criteria	Exclusion Criteria
<ul style="list-style-type: none"> ● Serosurvey in a defined geographic area representing a national or subnational geographic unit for which data on COVID deaths in all age groups are also available up to the date of the serosurvey. ● Sampling framework is defined. ● Sample sizes available for serosurvey, or uncertainty in the seroprevalence is explicitly quantified. ● Sero-assay sensitivity and specificity estimates available. ● At least 100 COVID-19 deaths observed in the study area by the serosurvey midpoint. ● First date of the serosurvey is before the introduction and widespread use of dexamethasone treatment (August 17, 2020)* 	<ul style="list-style-type: none"> ● Study participants selected based on being healthcare workers, having symptoms of COVID, referring themselves for a test or self-selection into the study (for example, choosing to go for an antibody test in a clinic or responding to an advert). ● Studies of outbreaks within a confined setting that does not include a representative sample of the general population (e.g. a school, a military ship). ● Studies exclusively or primarily in a narrow age group (e.g. school survey). ● Surveys of patients in clinical settings (assumed higher contact with health systems and healthcare workers).

2.1.2 Data Extraction and Collation

Observed seroprevalences, disaggregated by age and location where possible, were extracted from the manuscripts and other sources associated with the studies identified in the review. For the majority of studies (7/10), raw counts for the number of seropositives and number tested were available and extracted. However, this information was not available for three studies (conducted in Italy, Sweden and Denmark) and reported seroprevalence was extracted instead, alongside the stated confidence intervals. As a result, we used the reported confidence intervals to capture standard errors and used a logit-transformation instead of a binomial approach in our Age-Based model likelihood (**Age-Based Model Derivation**). Further uncertainties in the data extraction process include:

- For the Swedish study, seroprevalence data was extracted from public health reports that were being constantly updated and did not provide exact dates of the period in which the serostudy was conducted. It was therefore assumed that the serostudy was carried out in contiguous weeks across the study period, based on the provided figure in the report (accessed September 11, 2020).
- For the second seroprevalence survey carried out in the Netherlands, information was extracted from a news article (reporting an approximately 5.5% seropositivity among 7,000 participants: **Supplementary Table 2**). We therefore assumed there were 385/7,000 test-positives.
- In 5/10 studies (Zurich, Switzerland; Denmark; Sweden; Netherlands [second time point]), the age-specific seroprevalences were from broad age-groups or did not overlap well with reported death age-groups, only a national prevalence was available, or the report did not have sufficient detail to extract full information on sample sizes and seroprevalence. As a result, we assumed a constant attack rate (seroprevalence) across age-groups for these studies.

In addition to extracting this seroprevalence data, we also collated additional data required to estimate the IFR. These included:

(1) Daily time-series of COVID-19 deaths were preferentially obtained from the relevant Ministries of Health and other national public health agencies (further details in **Supplementary Table 2**). In some instances when this data was not available, daily deaths were extracted from the COVID-19 Data Repository by the Center for Systems Science and Engineering at Johns Hopkins University^{2,3} (and to which we applied a lagged difference to convert the cumulative counts to daily incidence). In a limited number of cases, Ministries of Health have retrospectively removed previously reported deaths, leading to negative reported deaths on particular days - these observations were set to zero. This age-aggregated data (*i.e.* deaths summed across age-groups) was used in the absence of age-specific COVID-19 death time series data being available.

(2) The proportion of COVID-19 deaths occurring by age in each location, again extracted from official reports put out by Ministries of Health and public health agencies (detailed in **Supplementary Table 2**). We assume that the age distribution of deaths is constant over time.

(3) For 6/10 of studies (Denmark; England; Spain; Geneva, Switzerland; Zurich, Switzerland; New York State, USA) the proportion of overall deaths that occurred in care homes was available and extracted so that an adjusted IFR estimate excluding these deaths could be calculated. We assumed that all deaths attributed to care homes occurred among individuals aged 65-years or older. We assumed that seroprevalence across different age-groups was the same in the care home population as the general population (see main text for discussion of this).

(3A) In the Zurich study, over 40% of the daily observed deaths recorded a single death, which resulted in problems when rounding and trying to recalculate deaths occurring in the care homes. As a result, the adjusted IFR estimate excluding care home deaths for Zurich was not considered.

(4) Demographic data (*i.e.* age-specific population counts) were obtained from Ministries of Health and other national public health agencies (further details in **Supplementary Table 2**).

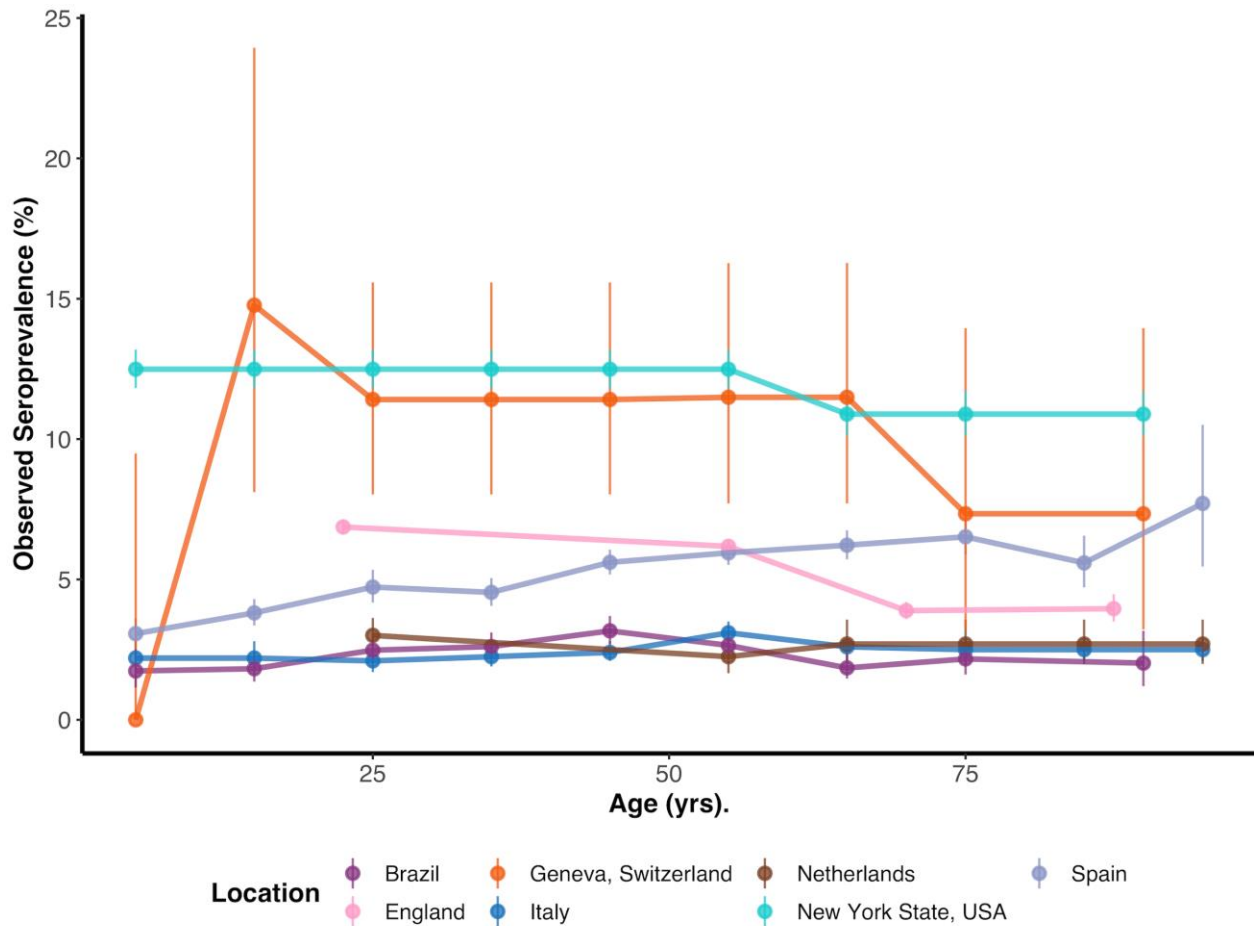
(5) Demographic data required in order to generate our standardized pooled IFR calculations for settings representative of each of the World Bank Income Strata - specifically Low Income Countries (LICs), Lower-Middle Income Countries (LMICs), Upper Middle Income Countries (UMICs) and High Income Countries (HICs). Consistent with previous analyses that have identified the representative countries in each of these strata ⁴, we selected Madagascar, Nicaragua, Grenada and Malta: information on their demographic structure was downloaded from the United Nations World Population Prospects 2019 site ⁵.

Supplementary Table 2 - Data Extraction Sources: The various sources of data for each respective study (reference numbers). For some regions, population demographic data was taken from the City Population (CP) website: <http://citypopulation.de/>

Study Location	Seroprevalence & Serovalidation Data	Number of Serostudy Timepoints	Age-Specific Death Data	Time-Series Death Data	Demographic Data	Care Home Death Source
Brazil	6,7	1	8	8	9, CP	-
Denmark	10,11	4	12	13	14	15
England	16,17	1	18	19	20	21
Italy [†]	22,23	1	22	24	25	-
Netherlands	26,27	2	28	29	30	-
Spain	31,32	3	33	33	34	15
Sweden	35,36*	8	37	38	39	-
Geneva, Switzerland	40,41	5	42	42	43	44
Zurich, Switzerland	45	2	42	42	43	44
New York State, USA	46	1	47	2,3	48	49

* Sweden seroprevalences were limited April 20 - June 12, 2020 when multiple regions were considered (Jämtland-Härjedalen, Jönköping, Kalmar, Skåne, Stockholm, Uppsala, Västerbotten, Västra Götaland, and Örebro). These provinces include the majority of the Swedish population and were assumed to be nationally representative.

[†] Serovalidation data has not yet been released for the Italy study. As a result, serovalidation data from a comparable study in San Francisco, USA, which used the same Abbot seroassay, were used as priors for the regional model and re-estimation of the test sensitivity and specificity.



Supplementary Figure 1 - Seroprevalence versus Age: Observed seroprevalence by age (mean age within each age-group plotted) and binomial proportion 95% confidence intervals for the seven studies where age-specific information was reported. With the exception of the Italian study (where reported seroprevalences and confidence intervals are plotted), the results presented are based on the raw number of individuals seropositive and number tested. The results of the latest seroprevalence survey are plotted among locations where multiple seroprevalence surveys had been conducted (except for the Netherlands where age specific seroprevalence was only available in the first survey). In our analysis we assumed a uniform seroprevalence across age-groups among the remaining three studies included that did not contain age-specific seroprevalence data.

2.2 Age-Based Statistical Model Derivation

2.2.1 Daily and age-stratified deaths

For individuals who die following infection, we assume that the time from infection to death follows a gamma distribution with shape α and rate β . If an individual is infected at time t then the probability that they die at time t_d is:

$$\Pr(t_d | t, \alpha, \beta) = \frac{\beta^\alpha}{\Gamma(\alpha)} (t_d - t)^{\alpha-1} e^{-\beta(t_d-t)}. \quad (1)$$

We make the simplifying assumption that time is discrete and measured in days, defining $\tau(T|t)$ to be the probability of death on day $T \in \mathbb{Z}_{>0}$ given infection at the start of day $t \in \mathbb{Z}_{>0}$ where $t \leq T$:

$$\tau(T | t) = \int_{T-1}^T \frac{\beta^\alpha}{\Gamma(\alpha)} (t_d - t + 1)^{\alpha-1} e^{-\beta(t_d-t+1)} dt_d \quad (2)$$

(the +1 term in the above comes about because we assume infections occur at the start of the day, but deaths can be registered until the end of the day, hence $\tau(1|1)$ returns a positive value).

Our population is split into different age strata, each with their own probabilities of infection and death. Let there be $A \in \mathbb{Z}_{>0}$ age groups in total, and let p_a be the proportion of the total population in age group $a \in 1:A$. In the simplest model we would expect infections to occur in a given age group in proportion to the number of people in that group. To allow for variation in age-specific attack rates, and in order to fit to age-specific seroprevalence data, we include a multiplicative attack rate scalar k_a within each group, allowing the final attack rate to be higher or lower than expected from proportions alone. Hence the overall probability of infection in age group a , which will be written ρ_a , is given by:

$$\rho_a = \frac{p_a k_a}{\sum_{i=1}^A p_i k_i}. \quad (3)$$

Once infected, the probability of death in age group a (i.e. the IFR in this age group) is defined as m_a . Hence, the overall probability of an individual in age group a dying on day T given infection on day t can be written $\rho_a m_a \tau(T|t)$.

Our raw data do not consist of individual-level outcomes, but rather aggregate counts. Specifically, two marginal distributions were available for each study: 1) daily counts of the number of COVID-19 deaths, summed over all age groups, and 2) the cumulative number of COVID-19 deaths at a single point in time, but broken down by age. Both marginal distributions were fit within a single statistical framework.

Let I_t be the number of new SARS-CoV-2 infections in the population on day t . The true infections curve is unknown, and was modelled using an exponentiated natural cubic spline, subject to the constraint that the total number infected (i.e. the area under the curve) could not exceed the total population size N . It follows from the definitions above that the number of infections in age group a on day t is given by $\rho_a I_t$,

and the number of ultimately fatal infections is given by $\rho_a m_a I_t$. The expected total deaths on day T , denoted μ_T , is obtained by summing over all age groups and all possible times of infection as follows:

$$\mu_T = \sum_{a=1}^A \rho_a m_a \sum_{t=1}^T I_t \tau(T | t). \quad (4)$$

The observed number of COVID-19 deaths on day T , denoted D_T , is assumed to be Poisson distributed around this expectation:

$$\Pr(D_T | \mu_T) = \frac{(\mu_T)^{D_T} e^{-\mu_T}}{D_T!}. \quad (5)$$

The likelihood for this part of the model is simply the product of Poisson probabilities over all days in our time series:

$$\mathcal{L}_1 = \prod_T \Pr(D_T | \mu_T). \quad (6)$$

Moving on to the second marginal distribution, the expected cumulative deaths in age group a up until time Y can be written:

$$q_a = \rho_a m_a \sum_{T=1}^Y \sum_{t=1}^T I_t \tau(T | t). \quad (7)$$

These expected values are converted into expected proportions of deaths in each age group as follows:

$$f_a = \frac{q_a}{\sum_{i=1}^A q_i}. \quad (8)$$

Finally, the observed cumulative COVID-19 deaths up until day Y , denoted by the vector \mathbf{C} with elements C_a for $a \in 1: A$, are assumed to be multinomially distributed with these proportions:

$$\Pr(\mathbf{C} | \mathbf{f}) = \left(\sum_{a=1}^A C_a \right)! \prod_{a=1}^A \frac{f_a^{C_a}}{C_a!}. \quad (9)$$

This is the second component of the likelihood:

$$\mathcal{L}_2 = \Pr(\mathbf{C} | \mathbf{f}). \quad (10)$$

2.2.2 Incorporating serology data

The third data type used in fitting comes from serological studies. For a given individual infected on day t we model the probability of having seroconverted by day t_s using the following formula:

$$\Pr(X = 1 | t_s, t, \lambda) = 1 - \exp\left(\frac{-(t_s - t)}{\lambda}\right), \quad (11)$$

where X is a binary variable that equals 1 if the individual has seroconverted and 0 otherwise. This is equivalent to assuming seroconversion with a constant hazard $1/\lambda$. Translating to the population level,

the expected number of people to have seroconverted by time T in age group a , denoted $\theta_{T,a}$, is given by:

$$\theta_{T,a} = \rho_a \sum_{t=1}^T I_t \Pr(X = 1 \mid T, t, \lambda). \quad (12)$$

This can be translated to an expected proportion via the expression $\theta_{T,a}/N_a$, where N_a is the total population size in age group a , such that $\sum_{a=1}^A N_a = N$.

The observed prevalence of seropositive individuals (the seroprevalence) is expected to deviate from this proportion due to both sampling effects and imperfect test characteristics. If $\gamma \in [0,1]$ is the sensitivity of the test and $\delta \in [0,1]$ is the specificity then the test-adjusted expected seroprevalence, $\phi_{T,a}$, can be calculated using the classic Rogan-Gladen correction⁶⁴:

$$\phi_{T,a} = \gamma \left(\frac{\theta_{T,a}}{N_a} \right) + (1 - \delta) \left(1 - \frac{\theta_{T,a}}{N_a} \right). \quad (13)$$

Let the total number of people tested on day T in age group a be denoted $s_{T,a}$, and let the observed number of seropositives be denoted $n_{T,a}$. We model the observed counts as binomially distributed around the Rogan-Gladen-corrected proportion:

$$\Pr(n_{T,a} \mid \phi_{T,a}) = \binom{s_{T,a}}{n_{T,a}} \phi_{T,a}^{n_{T,a}} (1 - \phi_{T,a})^{s_{T,a} - n_{T,a}}. \quad (14)$$

Finally, the likelihood for this component of the model is the product of the binomial probability over all age groups, and over all serology study dates T_y :

$$\mathcal{L}_3 = \prod_y \prod_{a=1}^A \Pr(n_{T_y,a} \mid \phi_{T_y,a}). \quad (15)$$

2.2.3 Extension for seroreversion

As part of a sensitivity analysis, we allowed for individuals to “serorevert” over time under an assumption of natural waning antibodies. We assumed that individuals experience a constant hazard $1/\lambda$ of seroconverting, followed by a probability of seroreverting characterized by a Weibull distribution with shape κ and scale μ . Under these conditions, the probability of being seropositive by the end of day t_s following infection on day t is given by:

$$\Pr(X = 1 \mid t_s, t, \lambda, \mu) = \int_t^{t_s} \frac{1}{\lambda} \exp \left(- \left(\frac{x-t}{\lambda} \right) - \left(\frac{t_s-x}{\mu} \right)^\kappa \right) dx. \quad (16)$$

All subsequent steps are identical to those described above in equations (12)-(15), resulting in an alternative version of the likelihood component \mathcal{L}_3 .

2.2.4 Full model

The full likelihood is the product of the individual likelihood components listed above:

$$\mathcal{L}_1 \mathcal{L}_2 \mathcal{L}_3 \quad (17)$$

3. Prior Information and Model Fitting

3.1 Symptom Onset to Seroreversion Parameter Estimation

We estimated the time to seroreversion (*i.e.* becoming antibody negative), from previously published longitudinal Abbott SARS-CoV-2 IgG assay data collected among non-hospitalized participants with real-time PCR-confirmed SARS-CoV-2 infections⁵⁰. We chose to estimate seroreversion times from the Abbott assay, as it showed the most striking decline in sensitivity over time compared to other serological assays⁵⁰. As a result, we present the most conservative IFR estimates with respect to the effects of seroreversion (*i.e.* the number of previously infected individuals, the IFR denominator, is inflated due to assumed “reverted” infections) to highlight the differences between estimates of IFR with and without the assumption of seroreversion to the greatest degree. All included participants had relatively mild COVID-19 disease and were not hospitalised. Of the 97 convalescent participants analyzed, three participants had missing information on days post-symptoms and were excluded. Of the remaining 94 participants, six did not seroconvert during follow-up (*i.e.* they were negative at baseline and remained so during the follow-up period). Among the final 88 participants, 62 were female and the median age was 48.5 years (range: 21 - 65 years). Seronegative status (*i.e.* the outcome) was defined as titres below an optical density of 1.4⁵⁰.

To estimate the time of seroreversion after symptom onset, we fit a Weibull survival model using interval censoring to account for the uncertainty in the observed time of seroreversion. As a comparison to our parametric fit, we also fit a Kaplan-Meier survival curve with interval-censoring. Models were fit using the `survival` R-package^{51,52}. The `survminer` R-package was used in plotting the Kaplan-Meier survival curve (**Figure 1A**)⁵³.

From the Weibull survival model, we found that the Weibull shape and scale parameters were 3.67 and 143.7, respectively. In order to conform with the mathematical derivation of the model (**Equation 16** above), we subtracted 13.3 (days) from the Weibull scale parameter to account for the time of symptom onset to seroconversion (as an approximation)⁵⁴.

3.2 Onset-Outcome Delay Distributions and Serological Test Characteristics

The delay from onset of symptoms to death was assumed to follow a gamma distribution with a mean of 14.8 days and coefficient of variation of 0.85 (unpublished data from the COVID-19 Hospitalisation in England Surveillance System and Public Health England). The delay from onset of symptoms to seroconversion was assumed to follow an exponential distribution with a mean time of seroconversion of 13.3 days⁵⁴. For both distributions, the incubation period was assumed to be fixed at five days^{55,56}, thereby providing overall means of onset of infection to death and seroconversion of 19.8 and 18.3 days, respectively. Priors for the onset-delay means were truncated Gaussian distributions while the onset-to-death coefficient of variation had a Beta distributed prior (**Supplementary Table 3**). When seroreversion was considered, the prior for rate of seroreversion after seroconversion was assumed to have a truncated Gaussian distribution (**Supplementary Table 3**).

The prior distributions for the sensitivity and specificity were assumed to follow Beta distributions with the number of true positives that were correctly identified considered for sensitivity, and the number of true negatives correctly identified considered for specificity, among the total number of samples tested (**Supplementary Table 3**). To allow for some uncertainty -- even among studies that found 100% specificity during serovalidation -- we added 0.5 to our Beta scale and shape parameters (the Jeffreys prior; **Supplementary Table 3**). For the subset of studies where regional seroprevalence information was available (6/10), we used the posterior estimates of sensitivity and specificity from the region-based models without time delays to re-inform the priors for the age-based IFR model. The new Beta distribution shape parameters were calculated from the regional-based model sensitivity and specificity posteriors using a method of moments approach with `fitdistplusr` R-package⁵⁷ (**Supplementary Table 7**).

The prior distributions for the age-specific IFR estimates were assumed to be uniform with minimum and maximum values of 0% and 40%, respectively. The 40% maximum was selected as not more than three-times the upper credible interval of three early IFR studies⁵⁸⁻⁶⁰ (**Supplementary Table 3**).

Spline curves were fit with five knots to estimate the incidence of infections over time, with uniform priors on the x- and y-axis positions. The minimum and maximum values of the y-axis positions were zero and the total population size, while the maximum x-axis position was allowed to range from fourteen days prior to the last observed death date and the last observed death date, respectively (**Supplementary Table 3**).

To estimate the proportion of infections occurring in each age group, we assumed that the attack rate was proportional to the population fraction within that age group multiplied by an additional scaling parameter assumed to follow a truncated Gaussian distribution (**Supplementary Table 3**). The modelled seroprevalence by age was fit to the age specific seroprevalence data. Given that serostudies were conducted over a given timeframe (*e.g.* two-weeks), we took the average of the model seroprevalences over the serostudy time-period to propagate uncertainty in collection times. These modelled prevalences were then compared with the reported seroprevalence.

Models were fit using Metropolis-Coupled Markov Chain Monte Carlo (MC³) with the `drjacoby` R package⁶¹. For each model, 10,000 burnin-in and 10,000 sampling iterations with 50 rungs across 10 chains were considered. The thermodynamic power between rungs was sequentially ranged from 5.0 to 2.5 for all sites except England and Spain, where the thermodynamic power was ranged from 5.0 to 3.5, to ensure high swap rates. Model convergence was assessed by analyzing the acceptance rate between rungs, visualization of chains, and a Gelman-Rubin's convergence diagnostic lower than 1.1⁶².

Supplementary Table 3 - Prior Distributions used in Age-Specific Model: For each parameter, the prior distribution is indicated alongside the parameter count. For the age-specific infection fatality ratios (IFRs), younger age-groups were reparameterized as relative risk to the oldest age group in order to improve model mixing. Similarly, the spline knots were reparameterized relative to the last observed day, where E was the last observed day and $E-14$ was fourteen days prior. The first knot was always fixed at one to allow for a common time origin. The spline y -positions were similarly set relative to the third y -position, which was allowed to range between zero and the approximate size of the population (popN).

Parameter	Count	Distribution
Age-Specific IFRs	Number of Age Groups	Uniform(0,1); Uniform(0, 0.4)
Knots	5	Uniform(0,1); Uniform($E-14$, E)
Spline Y-Positions	5	Uniform(0,1); Uniform(0, popN)
Attack Rate Noise Scalars	Number of Age Groups	Truncated-Normal(1, 0.05) Bounds: 0.5, 1.5
Mean of Onset from Infection to Seroconversion	1	Truncated-Normal(18.3, 0.1) Bounds: 16, 21
Mean of Onset from Infection to Death	1	Truncated-Normal(19.8, 0.1) Bounds: 18, 20
Coefficient of Variation of Onset from Infection to Death	1	Beta(2550, 450)
Weibull Shape Pattern for Seroreversion	1	Truncated-Normal(3.67, 0.5) Bounds: 2, 5
Weibull Scale Pattern for Seroreversion	1	Truncated-Normal(130.4, 0.1) Bounds: 127, 133

3.3 Estimating Specificity: Region-based Statistical Model Description

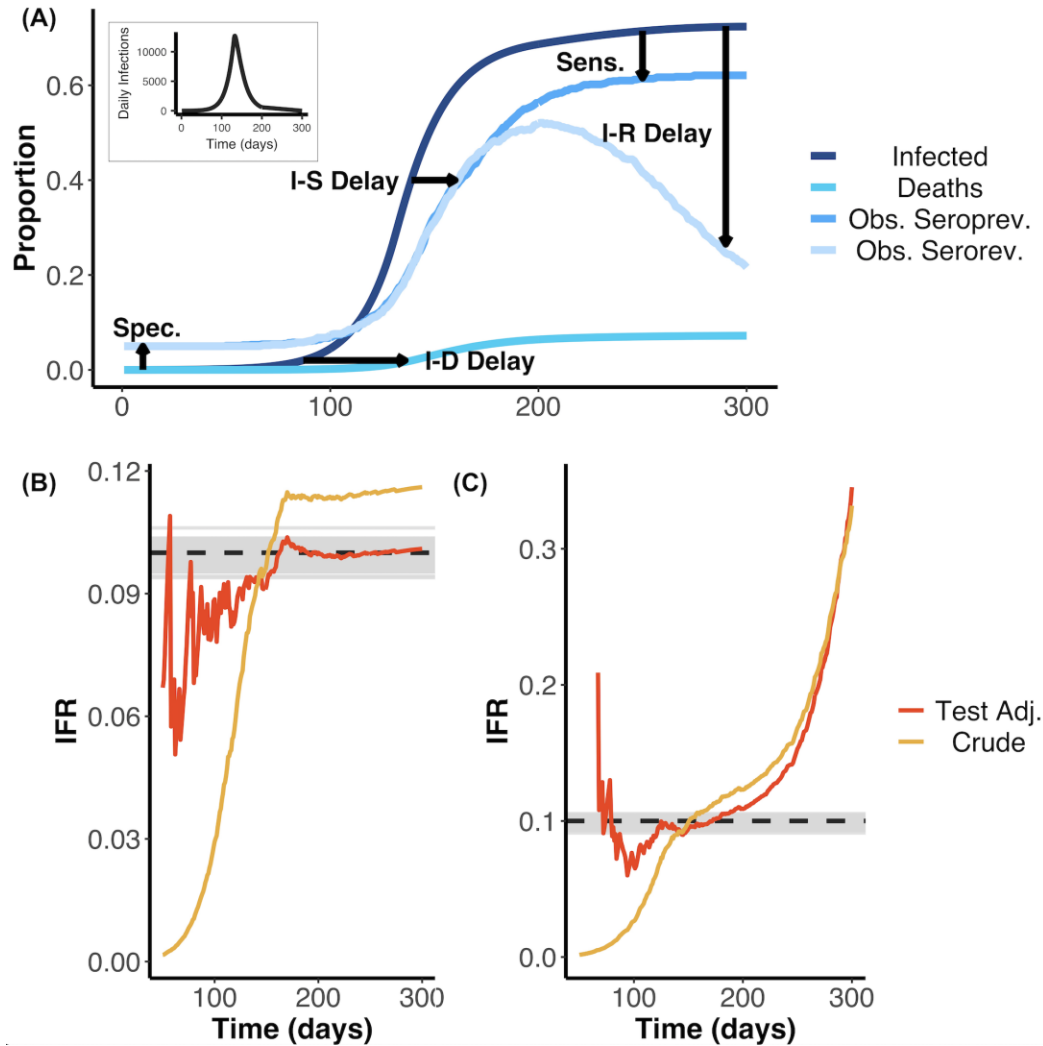
An adapted version of the statistical model described above was used to estimate serological test specificity in six studies where data were available by region within the larger serosurvey, as described in the main text. The underlying assumption is that deaths in each region are proportionally related to the true cumulative incidence in the region, estimated by seroprevalence, after adjusting for serological test performance. As before, we incorporated test sensitivity and specificity into this model using the reported validation data from each study as priors, and we then estimated regional and age-specific seroprevalence, specificity, sensitivity and deaths. The age-specific IFRs were assumed to be the same in each region, but incorporated region-specific demography so that the overall regional IFRs could vary (e.g. London, England has a much younger population than the rest of the country, and therefore a lower overall IFR). The delays from onset-death and onset-seroconversion were removed for analytical tractability, and we used cumulative mortality data up to the midpoint of the serosurvey, making the assumption that most deaths and seroconversion had occurred by the time of the serosurvey. This assumption is reasonable for serosurveys conducted some weeks after the first wave of the epidemic. We did not have seroprevalence data broken down by both age and region at the same time, but we fit the model to both the marginal age and regional seroprevalence, assuming the same risk ratios of being seropositive by age in all regions. We did not include seroreversion in this analysis. The model was fit with `RStan` using 4 chains, each having 10,000 burn-in and 10,000 sampling iterations⁶³. Convergence was assessed by visualizing the posterior distributions as well as requiring Gelman-Rubin's convergence diagnostic lower than 1.1⁶². The underlying code is available on Github ([mrc-ide/reestimate_covidIFR_analysis/analyses/Rgn_Mod_Stan](https://github.com/mrc-ide/reestimate_covidIFR_analysis/analyses/Rgn_Mod_Stan)).

4. Insights from Simulated Data

Accurate inference of the IFR based on serological data is challenging due to a number of factors that can bias estimates away from the true value. These factors include: (1) the delay between infection and death, (2) the dynamical process of seroconversion and seroreversion, and (3) serological test characteristics -- all of which are expected to interact leading to complex effects on the IFR. In order to understand how these factors might bias the IFR, and understand the extent to which they could be disentangled, we first developed a statistical simulator that modelled these factors and their respective effects on the IFR.

From simulations assuming seroconversion without seroreversion, we found that the crude IFR tended to underestimate the true IFR when the epidemic was growing, or overestimate the true IFR when the epidemic was contracting. Moreover, even after adjusting the IFR for test performance using the Rogan-Gladen correction, a common approach to adjust for test sensitivity and specificity⁶⁴, the true IFR was only captured when the epidemic was nearly over (**Supplementary Figure 2A**). These biases result from failing to account for the delays from onset of infection to death and seroconversion. When considering the possibility of seroreversion after seroconversion, we found that after the epidemic peaked, both the crude IFR and the tested-adjusted IFR increasingly overestimated the true IFR as more time passed from the first wave of the epidemic to when the serological study was undertaken (**Supplementary Figure 2B**). This underestimation is expected, since reducing seroprevalence deflates the denominator (*i.e.* total number infected) while the numerator (*i.e.* cumulative deaths) remains constant or increases.

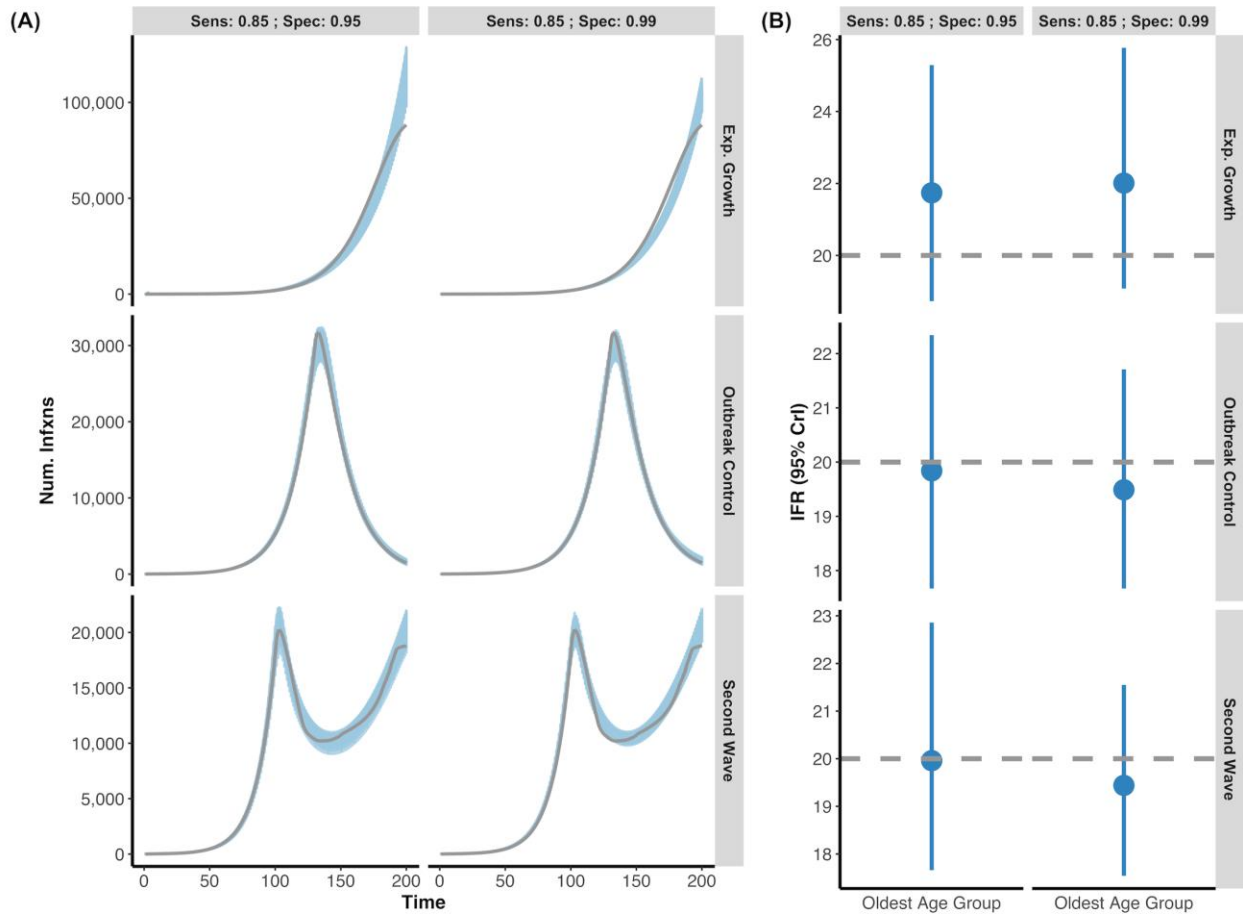
Following our better understanding of these biases, we developed a statistical framework that accounted for onset-outcome delay distributions alongside serologic test characteristics (*e.g.* specificity, sensitivity, and the duration of the serosurvey). We found that our model allowed for correct inference of the simulated true IFR when the potentiality for seroreversion was not and was considered (**Supplementary Figure 2**). Full details on this Age-Based model framework and its mathematical derivation are detailed above.



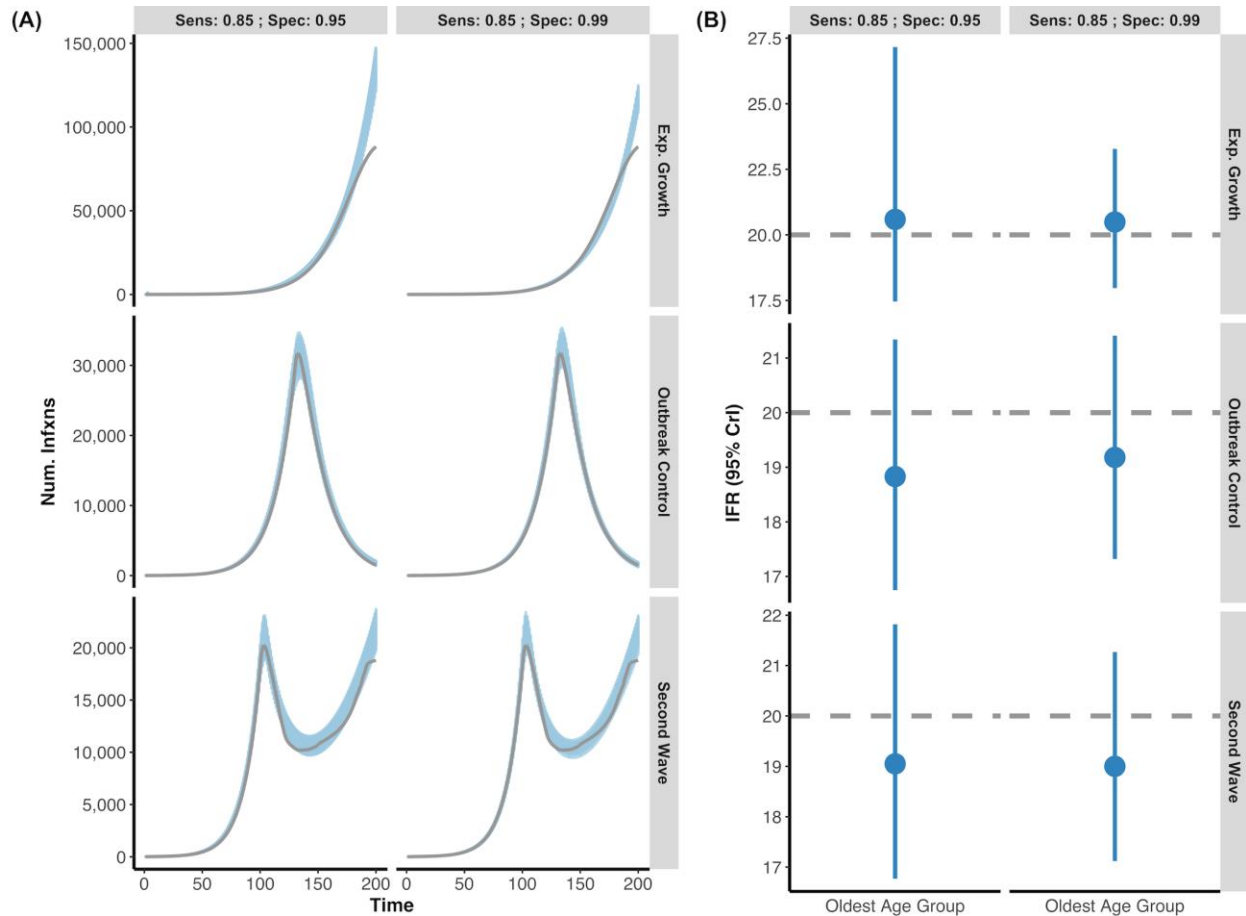
Supplementary Figure 2: (A) Schematic illustrating how the effects of the various factors needed to correctly infer the IFR can bias crude and test-adjusted (Test Adj.) estimates of the IFR. Factors shown include delays from infection to death (I-D), to seroconversion (I-S), and to seroreversion (I-R) as well as serological test sensitivity (Sens), and specificity (Spec). Seroprevalence was simulated from days 145-155 and 195-205 using a serologic test with 95% specificity and 85% sensitivity and assuming that 0.1% of the total population was sampled. These simulations, without and with seroreversion, were used as the inputs for the results displayed in panels (B) and (C). The daily infection curve used as input for the simulation is shown as the plot inset. (B) Estimated IFR over time based on fitting a statistical model to the simulated data that does not include seroreversion. Here, the underlying true IFR associated with the simulated data is indicated by the dashed black line and the grey lines indicate 100 posterior draws from the fitted statistical model (based on the posterior probability), indicating the capacity for our model framework to correctly recover the true IFR. Red and yellow lines represent the crude and test characteristic-adjusted (Rogan-Gladen correction) IFR estimates, calculated as if the serosurvey had been conducted on each respective day (after day 50). The crude IFR calculation did not include cumulative deaths in the denominator (see main text). (C) As for (B), but fitting a model that included seroreversion instead of one that lacked this feature. The IFR values are shown as a probability instead of a percentage. Early in the outbreak, when the true seroprevalence is less than the false positive rate, adjusting for the serologic test characteristics can result in unstable IFR estimates.

Supplementary Figure 2 highlights the capacity for our statistical framework to recover the true underlying IFR for a simple epidemic. We next assessed whether our model was robust to more complex epidemic shapes. Infection curves were simulated with three shapes: exponential (unmitigated) growth, exponential growth followed by interventions that led to resolution of the outbreak, and exponential growth followed by interventions that lead to a nadir but were followed by a “second wave” as interventions were relaxed. These simulations are respectively referred to as the Exponential Growth, Outbreak Control, and Second Wave scenarios. Simulations were assumed to have two observed seroprevalence time points (Midday: 125 and 175, where simulated serostudies were conducted over ten days). In each instance, we found that our age-specific IFR model was able to capture the simulated true IFR value within the 95% credible interval when seroreversion was and was not considered (**Supplementary Figures 3-4**). Overall, the model appeared to be most sensitive to the unmitigated exponential growth scenario, where the number of infections was slightly underestimated in some posterior draws. In some instances, this resulted in the younger age groups having IFRs that were slightly over-estimated (*e.g.* 0.11-0.14% instead of 0.1%) whilst the older age-groups’ true IFR was always captured by the 95% credible intervals. This is due to the fact that the delay of onset of infection to death results in a “lagged” infection curve, where those infected have not yet died and there is little information to fit to a continued exponential growth versus any other shape (*e.g.* a continued linear line, a plateau, etc.), particularly when there are very few deaths in the younger age-groups.

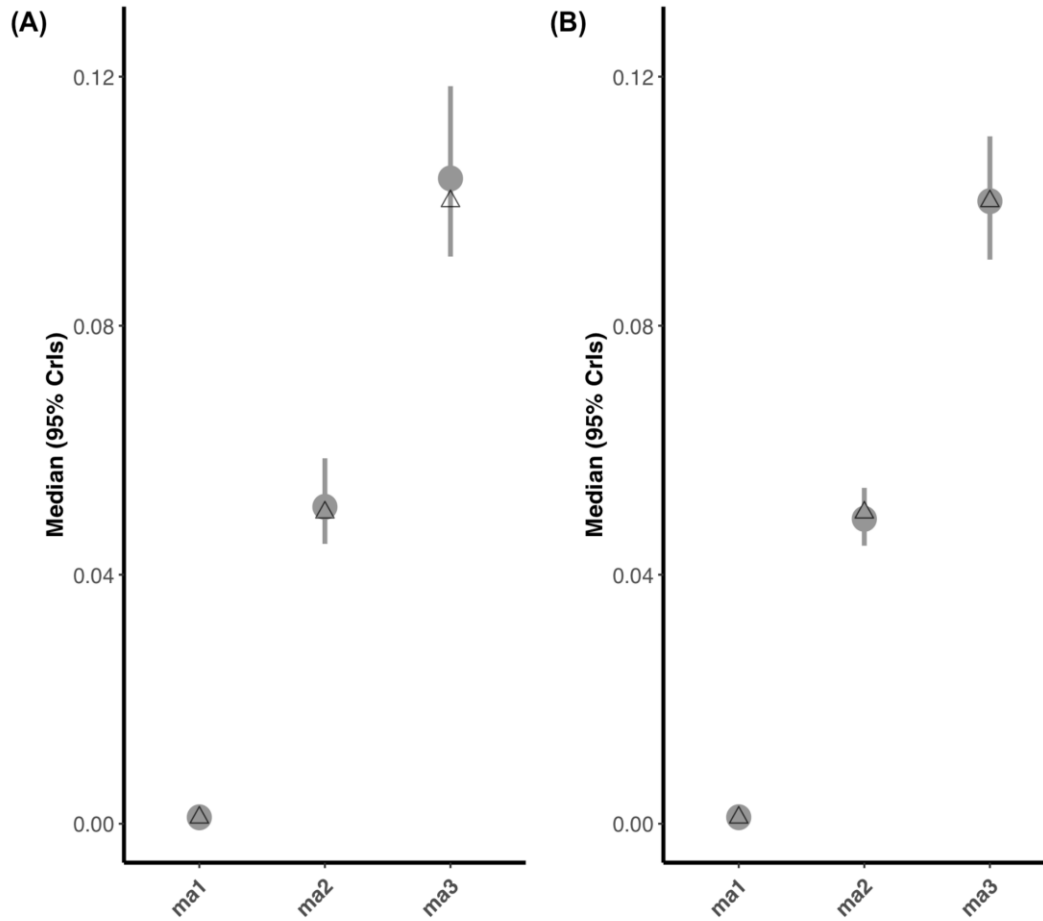
Additionally, we show that our age-specific IFR model remains able to capture the true underlying IFR in simulated data when only a single serostudy day is considered, rather than the two sequential serostudies assumed for the Supplementary Figure 3 and 4 results (**Supplementary Figure 5**). The results in **Supplementary Figure 5** show that the uncertainty in the IFR estimates is often increased when only a single serostudy day is considered.



Supplementary Figure 3 - Posterior Draws of Several Epidemic Shapes versus Simulated Infection Curve without Seroreversion: (A) Using simulated data, we created three outbreak scenarios where individuals who seroconverted could not serorevert: exponential growth, outbreak control, and second wave (grey lines are simulated infection input) under two different serological tests (Sensitivity: 85%; Specificity 95% vs. Sensitivity: 85%; Specificity 99%). The blue shading represents 100 posterior draws (based on the posterior probability) of the modelled infection curve (using an exponentiated natural cubic spline), where draws were selected based on their posterior probability. **(B)** The inferred median and 95% credible intervals (blue) versus the simulated true IFR (grey, dashed line) for each of the scenarios under the two serological test characteristics. Overall, the model accurately captures both the simulated infection curve and the simulated IFR despite complex epidemic shapes. For all epidemic scenarios considered, we assume that there are two seroprevalence surveys that range over days 120-130 and 170-180 and that 0.1% of the population was sampled.



Supplementary Figure 4 - Posterior Draws of Several Epidemic Shapes versus Simulated Infection Curve with Seroreversion: (A) Simulated data representing the same three outbreak scenarios featured in Supplementary Figure 3 (exponential growth, outbreak control, and second wave) were generated, but now with the additional feature that individuals who seroconverted could potentially serorevert. Grey lines indicate the simulated true infection curve under two different serological tests (Sensitivity: 85%; Specificity 95% vs. Sensitivity: 85%; Specificity 99%). The blue shading represents 100 posterior draws (based on the posterior probability) of the modelled infection curve (using an exponentiated natural cubic spline), where draws were selected based on their posterior probability. (B) The inferred median and 95% credible intervals (blue) versus the simulated true IFR (grey, dashed line) for each of the outbreak scenarios with respect to the two different serological test characteristics. As above, the model accurately captures both the simulated infection curve and the simulated IFR while accounting for the potentiality of seroreversion. For all epidemic scenarios considered, we assume that there are two seroprevalence surveys that range over days 120-130 and 170-180 and that 0.1% of the population was sampled.



Supplementary Figure 5 - Comparison of the Number of Serosurveys: Data was simulated for three age-groups (ma1, ma2, ma3) with IFRs of 0.1%, 1%, and 10%, respectively. Follow-up time was assumed to be 200-days. The simulations differed in the number of serological time points considered (*i.e.* simulated serosurveys) with (A) consisting of a single serosurvey ranging from days 145-155 versus (B) consisting of two serosurveys: days 120-130 and 170-180, respectively. In both simulations, we assume that 0.1% of the population was sampled and that the simulated serologic test had a sensitivity and specificity of 0.85% and 0.95%, respectively. Although both models capture the true simulated IFR values in the 95% credible intervals (grey) for each age group, there is greater uncertainty when only a single serosurvey is considered. The IFR values are shown as a probability instead of a percentage.

5. Age-Based Statistical Model Posteriors

5.1 Posterior Parameter Estimates

Supplementary Table 4- Overall IFR Estimates when Standardized by Population Demography and Inferred Attack Rates: The overall IFR estimates were calculated by standardizing for demography and the inferred attack rate, following the definition from the age-based model (columns 3-4) or by standardizing for solely the demography and assuming the same attack rate in each age-group (columns 5-6). Generally, the overall IFRs were very similar between the two approaches with England as a notable exception, where the lower attack rate in the oldest age group (consistent with the seroprevalence data) drove down the IFR.

Study Location	Crude IFR (95 CrI%)	Pop.-Attack Standardized Modelled IFR without Seroreversion (95% CrI)	Rate Pop.-Attack Standardized Modelled IFR with Seroreversion (95% CrI)	Pop. Standardized Modelled IFR without Seroreversion (95% CrI)	Rate Pop. Standardized Modelled IFR with Seroreversion (95% CrI)
Brazil	0.99 (0.92, 1.06)	1.03 (0.93, 1.17)	0.99 (0.89, 1.13)	1.05 (0.95, 1.21)	1.01 (0.91, 1.17)
Denmark	0.33 (0.23, 0.48)	0.53 (0.37, 1.01)	0.52 (0.37, 0.99)	0.53 (0.38, 1.02)	0.52 (0.37, 0.98)
England	1.41 (1.38, 1.45)	1.18 (0.99, 1.34)	1.04 (0.84, 1.19)	1.53 (1.26, 1.79)	1.34 (1.07, 1.55)
Italy	2.3 (1.94, 2.72)	2.53 (2.31, 2.77)	2.23 (2.03, 2.45)	2.53 (2.3, 2.79)	2.23 (2.02, 2.46)
Netherlands	0.6 (0.58, 0.63)	0.62 (0.58, 0.68)	0.59 (0.55, 0.66)	0.62 (0.58, 0.68)	0.6 (0.56, 0.66)
Spain	1.12 (1.08, 1.16)	1.14 (1.08, 1.22)	1.07 (1.01, 1.14)	1.04 (0.97, 1.12)	0.98 (0.91, 1.05)
Sweden	0.68 (0.46, 1)	1.03 (0.88, 1.37)	0.99 (0.84, 1.35)	1.03 (0.87, 1.37)	0.99 (0.84, 1.36)
Geneva, Switzerland	0.48 (0.42, 0.56)	0.49 (0.42, 0.59)	0.48 (0.4, 0.58)	0.52 (0.43, 0.63)	0.5 (0.42, 0.61)
Zurich, Switzerland	0.51 (0.45, 0.58)	0.52 (0.41, 0.67)	0.5 (0.39, 0.64)	0.53 (0.41, 0.67)	0.5 (0.39, 0.65)
New York State, USA	0.75 (0.74, 0.76)	0.77 (0.72, 0.83)	0.75 (0.7, 0.8)	0.82 (0.77, 0.89)	0.8 (0.74, 0.86)

Supplementary Table 5 - Delay Distribution Posteriors: The posterior 95% credible intervals (CrI) for the mean delay from infection onset to seroconversion (Serocon.) and death as well as the coefficient of variation (Coeff. of Variation) for the onset of infection to death gamma distribution are shown for each study when seroconversion was not and was considered. Similarly, the mean of the onset from seroconversion to seroreversion (Serorev.) posterior distribution is given for fits where seroreversion was modelled.

Study Location	Model Consideration	Onset to Serocon. Mean (95% CrI)	Onset to Death Mean (95% CrI)	Onset to Death Coeff. of Variation (95% CrI)	Serocon. to Serorev. Mean (95% CrI)
Brazil	Without Serorev.	18.3 (18.11, 18.5)	19.76 (19.56, 19.95)	0.85 (0.84, 0.86)	
Brazil	With Serorev.	18.3 (18.1, 18.49)	19.76 (19.57, 19.95)	0.85 (0.84, 0.86)	132.97 (132.85, 133)
Denmark	Without Serorev.	18.3 (18.1, 18.5)	19.8 (19.61, 19.97)	0.85 (0.84, 0.86)	
Denmark	With Serorev.	18.3 (18.11, 18.5)	19.8 (19.61, 19.97)	0.85 (0.84, 0.86)	132.88 (132.37, 133)
England	Without Serorev.	18.3 (18.11, 18.5)	19.79 (19.59, 19.96)	0.87 (0.85, 0.88)	
England	With Serorev.	18.3 (18.1, 18.5)	19.79 (19.59, 19.96)	0.87 (0.85, 0.88)	132.95 (132.71, 133)
Italy	Without Serorev.	18.3 (18.1, 18.5)	19.87 (19.69, 19.99)	0.86 (0.85, 0.87)	
Italy	With Serorev.	18.3 (18.11, 18.5)	19.87 (19.69, 19.99)	0.86 (0.85, 0.87)	132.93 (132.61, 133)
Netherlands	Without Serorev.	18.31 (18.11, 18.51)	19.8 (19.6, 19.96)	0.85 (0.84, 0.86)	
Netherlands	With Serorev.	18.31 (18.11, 18.51)	19.8 (19.6, 19.97)	0.85 (0.84, 0.86)	130.4 (130.21, 130.6)
Spain	Without Serorev.	18.29 (18.1, 18.49)	19.71 (19.53, 19.88)	0.84 (0.83, 0.85)	
Spain	With Serorev.	18.3 (18.11, 18.49)	19.71 (19.52, 19.88)	0.84 (0.83, 0.85)	132.26 (129.24, 132.97)
Sweden	Without Serorev.	18.3 (18.11, 18.5)	19.79 (19.6, 19.96)	0.85 (0.84, 0.86)	
Sweden	With Serorev.	18.3 (18.11, 18.5)	19.79 (19.6, 19.96)	0.85 (0.84, 0.86)	130.41 (130.21, 130.6)
Geneva, Switzerland	Without Serorev.	18.3 (18.11, 18.5)	19.77 (19.57, 19.95)	0.85 (0.84, 0.86)	
Geneva, Switzerland	With Serorev.	18.3 (18.11, 18.5)	19.77 (19.57, 19.95)	0.85 (0.84, 0.86)	130.4 (130.21, 130.6)
Zurich, Switzerland	Without Serorev.	18.3 (18.1, 18.49)	19.79 (19.59, 19.96)	0.85 (0.84, 0.86)	
Zurich, Switzerland	With Serorev.	18.3 (18.1, 18.49)	19.79 (19.6, 19.96)	0.85 (0.84, 0.86)	130.4 (130.21, 130.6)
New York State, USA	Without Serorev.	18.3 (18.1, 18.49)	19.74 (19.55, 19.94)	0.87 (0.86, 0.89)	
New York State, USA	With Serorev.	18.3 (18.1, 18.49)	19.75 (19.55, 19.93)	0.87 (0.86, 0.88)	132.81 (131.98, 132.99)

Supplementary Table 6- Age Specific Estimates of the Infection Fatality Ratio across Included Studies: The age-specific IFR estimates (without standardization) are provided with 95% credible intervals (CrI) for models where seroconversion was not and was considered. The crude IFRs and 95% confidence intervals (CI) are included for comparison. In addition, the inferred observed seroprevalence -- from 100 posterior draws based on the posterior probabilities and corrected for test sensitivity and specificity with the Rogan-Gladen equation -- is provided alongside the observed seroprevalence for the latest serosurvey with respect to each study and age-group. Ages of "999" indicate an upper bound.

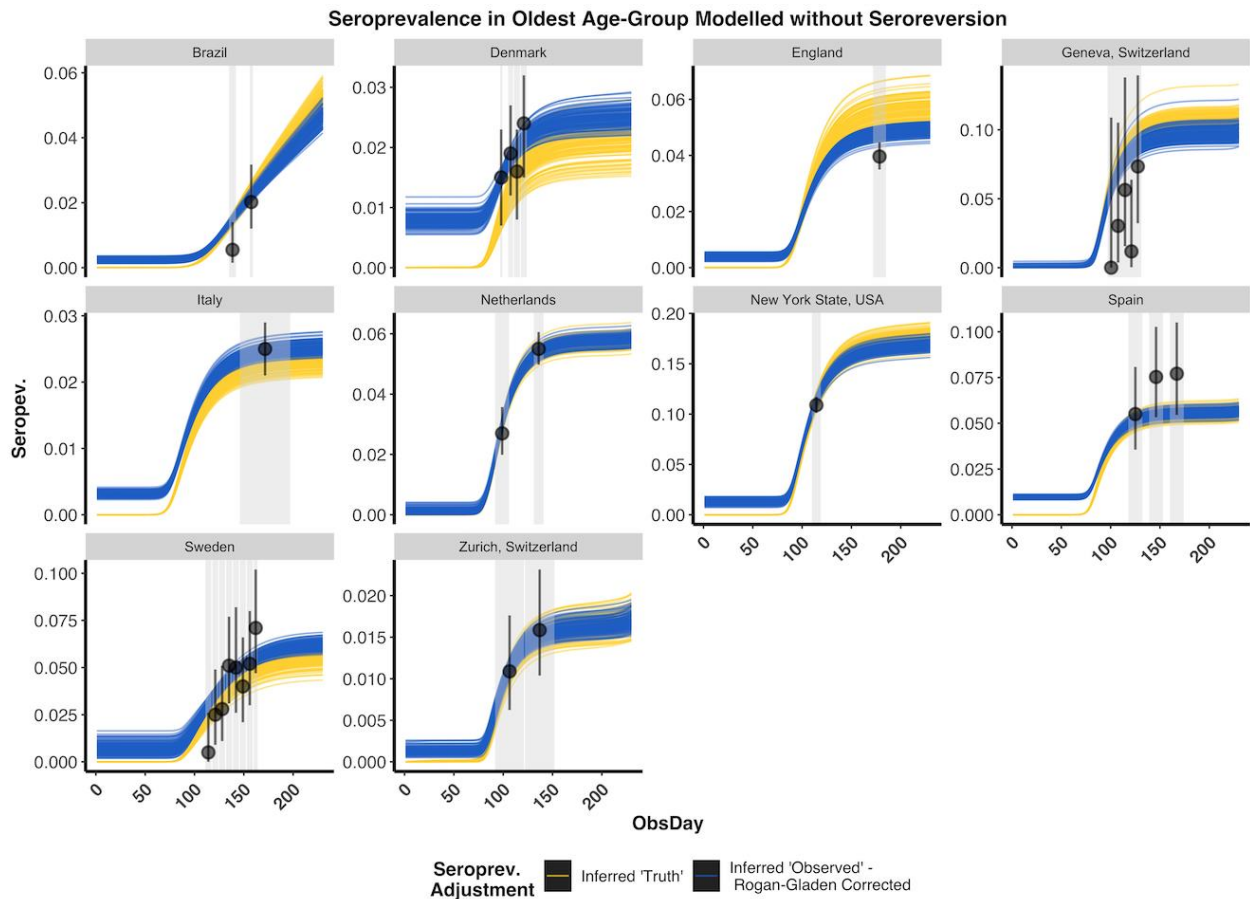
Study Location	Age Group (years)	Seroprev. Midday	Observed Seroprev.	Modelled Seroprev. without Serorev.	Modelled Seroprev. with Serorev.	Crude IFR (95% CI)	IFR Serorev. (95% CrI)	IFR without Serorev. (95% CrI)	IFR with Serorev. (95% CrI)
Brazil	(0,9]	2020-06-06	1.74	2.24 (2.07, 2.42)	2.23 (2.07, 2.42)	0.03 (0.02, 0.05)	0.03 (0.02, 0.03)	0.02 (0.02, 0.03)	
Brazil	(9,19]	2020-06-06	1.82	2.23 (2.09, 2.41)	2.22 (2.08, 2.39)	0.03 (0.02, 0.04)	0.02 (0.02, 0.03)	0.02 (0.02, 0.02)	
Brazil	(19,29]	2020-06-06	2.48	2.31 (2.16, 2.47)	2.32 (2.15, 2.51)	0.06 (0.05, 0.08)	0.07 (0.06, 0.08)	0.07 (0.06, 0.08)	
Brazil	(29,39]	2020-06-06	2.61	2.34 (2.17, 2.51)	2.34 (2.17, 2.48)	0.19 (0.16, 0.22)	0.2 (0.18, 0.24)	0.2 (0.17, 0.23)	
Brazil	(39,49]	2020-06-06	3.17	2.44 (2.3, 2.61)	2.44 (2.28, 2.63)	0.39 (0.33, 0.46)	0.49 (0.43, 0.57)	0.47 (0.41, 0.55)	
Brazil	(49,59]	2020-06-06	2.65	2.38 (2.24, 2.56)	2.39 (2.22, 2.56)	1.06 (0.9, 1.27)	1.17 (1.03, 1.36)	1.13 (0.99, 1.31)	
Brazil	(59,69]	2020-06-06	1.85	2.15 (1.98, 2.3)	2.15 (2.01, 2.29)	3.61 (2.96, 4.56)	3.18 (2.8, 3.7)	3.06 (2.67, 3.57)	
Brazil	(69,79]	2020-06-06	2.17	2.23 (2.08, 2.42)	2.25 (2.11, 2.43)	6.25 (4.93, 8.32)	6.31 (5.49, 7.39)	6.05 (5.27, 7.11)	
Brazil	(79,999]	2020-06-06	2.02	2.23 (2.02, 2.43)	2.24 (2.09, 2.45)	13.18 (9.19, 21.46)	13.47 (11.65, 16.13)	12.94 (11.22, 15.69)	
Denmark	(0,59]	30/04/2020	2.4	2.13 (1.9, 2.33)	2.11 (1.95, 2.39)	0.01 (0.01, 0.02)	0.02 (0.01, 0.04)	0.02 (0.01, 0.04)	
Denmark	(59,69]	30/04/2020	2.4	2.15 (1.89, 2.34)	2.12 (1.93, 2.39)	0.28 (0.19, 0.41)	0.45 (0.29, 0.88)	0.44 (0.28, 0.86)	
Denmark	(69,79]	30/04/2020	2.4	2.14 (1.88, 2.35)	2.1 (1.94, 2.4)	0.96 (0.66, 1.39)	1.57 (1.06, 3.03)	1.51 (1.03, 2.92)	
Denmark	(79,999]	30/04/2020	2.4	2.14 (1.86, 2.32)	2.12 (1.96, 2.37)	4.02 (2.79, 5.76)	6.76 (4.7, 13)	6.55 (4.58, 12.4)	
England	(0,44]	26/06/2020	6.87	6.62 (6.5, 6.78)	6.64 (6.42, 6.82)	0.02 (0.02, 0.02)	0.02 (0.02, 0.02)	0.02 (0.01, 0.02)	
England	(44,64]	26/06/2020	6.18	6.1 (5.91, 6.25)	6.1 (5.96, 6.23)	0.52 (0.5, 0.54)	0.45 (0.38, 0.51)	0.4 (0.32, 0.46)	
England	(64,74]	26/06/2020	3.89	4.38 (4.17, 4.64)	4.38 (4.23, 4.63)	3.19 (2.97, 3.45)	2.57 (2.13, 2.98)	2.25 (1.8, 2.65)	
England	(74,999]	26/06/2020	3.96	4.76 (4.46, 5.02)	4.8 (4.53, 5.14)	17.34 (15.75, 19.21)	15.06 (12.33, 17.82)	13.2 (10.47, 15.44)	
Italy	(0,9]	20/06/2020	2.2	2.41 (2.24, 2.57)	2.49 (2.3, 2.64)	0 (0, 0.01)	0 (0, 0.01)	0 (0, 0.01)	
Italy	(9,19]	20/06/2020	2.2	2.43 (2.21, 2.58)	2.49 (2.3, 2.7)	0 (0, 0)	0 (0, 0)	0 (0, 0)	
Italy	(19,29]	20/06/2020	2.1	2.39 (2.28, 2.56)	2.43 (2.27, 2.64)	0.01 (0.01, 0.01)	0.01 (0.01, 0.02)	0.01 (0.01, 0.02)	
Italy	(29,39]	20/06/2020	2.25	2.41 (2.26, 2.55)	2.46 (2.31, 2.63)	0.04 (0.04, 0.05)	0.04 (0.03, 0.06)	0.04 (0.03, 0.05)	

Italy	(39,49]	20/06/2020	2.4	2.45 (2.28, 2.62)	2.49 (2.34, 2.65)	0.14 (0.12, 0.16)	0.15 (0.13, 0.18)	0.13 (0.11, 0.16)
Italy	(49,59]	20/06/2020	3.1	2.64 (2.49, 2.77)	2.69 (2.53, 2.86)	0.4 (0.35, 0.46)	0.52 (0.46, 0.59)	0.46 (0.4, 0.52)
Italy	(59,69]	20/06/2020	2.6	2.47 (2.34, 2.66)	2.54 (2.37, 2.68)	1.75 (1.49, 2.04)	2.02 (1.78, 2.3)	1.78 (1.58, 2.03)
Italy	(69,79]	20/06/2020	2.5	2.47 (2.27, 2.67)	2.5 (2.34, 2.65)	5.64 (4.83, 6.55)	6.58 (5.83, 7.46)	5.82 (5.15, 6.57)
Italy	(79,89]	20/06/2020	2.5	2.47 (2.32, 2.61)	2.51 (2.32, 2.66)	12.47 (10.78, 14.3)	15.72 (13.95, 17.83)	13.89 (12.27, 15.74)
Italy	(89,999]	20/06/2020	2.5	2.46 (2.33, 2.6)	2.51 (2.36, 2.69)	19.44 (16.99, 22.03)	26.6 (23.56, 30.13)	23.46 (20.75, 26.66)
Netherlands	(0,49]	15/05/2020	5.5	5.49 (5.14, 5.87)	5.48 (5.21, 5.75)	0.01 (0.01, 0.01)	0.01 (0, 0.01)	0.01 (0, 0.01)
Netherlands	(49,59]	15/05/2020	5.5	5.38 (5.07, 5.62)	5.37 (5.04, 5.69)	0.11 (0.1, 0.12)	0.11 (0.09, 0.14)	0.11 (0.09, 0.13)
Netherlands	(59,69]	15/05/2020	5.5	5.45 (5.15, 5.72)	5.39 (5.15, 5.66)	0.45 (0.41, 0.5)	0.46 (0.41, 0.53)	0.44 (0.39, 0.5)
Netherlands	(69,79]	15/05/2020	5.5	5.43 (5.18, 5.7)	5.44 (5.15, 5.76)	2 (1.82, 2.21)	2.09 (1.89, 2.34)	2 (1.82, 2.25)
Netherlands	(79,89]	15/05/2020	5.5	5.47 (5.14, 5.71)	5.43 (5.17, 5.75)	6.38 (5.84, 7.01)	6.98 (6.35, 7.82)	6.69 (6.09, 7.48)
Netherlands	(89,999]	15/05/2020	5.5	5.42 (5.17, 5.67)	5.42 (5.11, 5.67)	10.65 (9.8, 11.65)	12.2 (10.9, 13.76)	11.7 (10.49, 13.22)
Spain	(0,9]	15/06/2020	3.07	3.76 (3.58, 3.98)	3.67 (3.48, 3.87)	0 (0, 0)	0 (0, 0.01)	0 (0, 0)
Spain	(9,19]	15/06/2020	3.81	4.38 (4.17, 4.56)	4.23 (4.03, 4.42)	0 (0, 0)	0 (0, 0.01)	0 (0, 0.01)
Spain	(19,29]	15/06/2020	4.73	5 (4.79, 5.17)	4.86 (4.65, 5.04)	0.01 (0.01, 0.02)	0.01 (0.01, 0.02)	0.01 (0.01, 0.02)
Spain	(29,39]	15/06/2020	4.54	4.91 (4.71, 5.1)	4.73 (4.56, 4.92)	0.03 (0.03, 0.04)	0.03 (0.02, 0.04)	0.03 (0.02, 0.04)
Spain	(39,49]	15/06/2020	5.61	5.67 (5.55, 5.82)	5.48 (5.35, 5.67)	0.07 (0.06, 0.07)	0.07 (0.06, 0.08)	0.06 (0.06, 0.07)
Spain	(49,59]	15/06/2020	5.95	5.93 (5.76, 6.1)	5.74 (5.59, 5.87)	0.21 (0.2, 0.23)	0.21 (0.19, 0.24)	0.2 (0.18, 0.22)
Spain	(59,69]	15/06/2020	6.22	6.07 (5.88, 6.25)	5.87 (5.67, 6.03)	0.73 (0.67, 0.79)	0.75 (0.69, 0.81)	0.7 (0.65, 0.77)
Spain	(69,79]	15/06/2020	6.52	6.18 (5.98, 6.35)	6 (5.77, 6.23)	2.46 (2.24, 2.72)	2.64 (2.44, 2.86)	2.48 (2.29, 2.69)
Spain	(79,89]	15/06/2020	5.59	5.55 (5.24, 5.89)	5.39 (5.15, 5.66)	7.78 (6.76, 9.1)	8.57 (7.81, 9.47)	8.03 (7.33, 8.85)
Spain	(89,999]	15/06/2020	7.71	5.56 (5.27, 5.88)	5.4 (5.14, 5.74)	10.05 (7.73, 13.85)	15.52 (13.97, 17.42)	14.56 (13.06, 16.36)
Sweden	(0,9]	2020-10-06	7.1	5.57 (5.15, 5.99)	5.47 (4.96, 5.83)	0 (0, 0)	0 (0, 0.01)	0 (0, 0.01)
Sweden	(9,19]	2020-10-06	7.1	5.54 (5.17, 5.96)	5.44 (5.08, 5.8)	0 (0, 0)	0 (0, 0)	0 (0, 0)
Sweden	(19,29]	2020-10-06	7.1	5.58 (5.19, 5.96)	5.41 (5.16, 5.9)	0.01 (0.01, 0.01)	0.01 (0.01, 0.03)	0.01 (0.01, 0.03)
Sweden	(29,39]	2020-10-06	7.1	5.59 (5.15, 5.9)	5.46 (5.1, 5.91)	0.01 (0.01, 0.02)	0.02 (0.01, 0.04)	0.02 (0.01, 0.04)
Sweden	(39,49]	2020-10-06	7.1	5.54 (5.2, 5.89)	5.44 (5.11, 5.87)	0.05 (0.03, 0.07)	0.08 (0.05, 0.11)	0.07 (0.05, 0.11)
Sweden	(49,59]	2020-10-06	7.1	5.57 (5.19, 5.92)	5.43 (5.04, 5.82)	0.17 (0.11, 0.25)	0.26 (0.2, 0.35)	0.25 (0.19, 0.34)

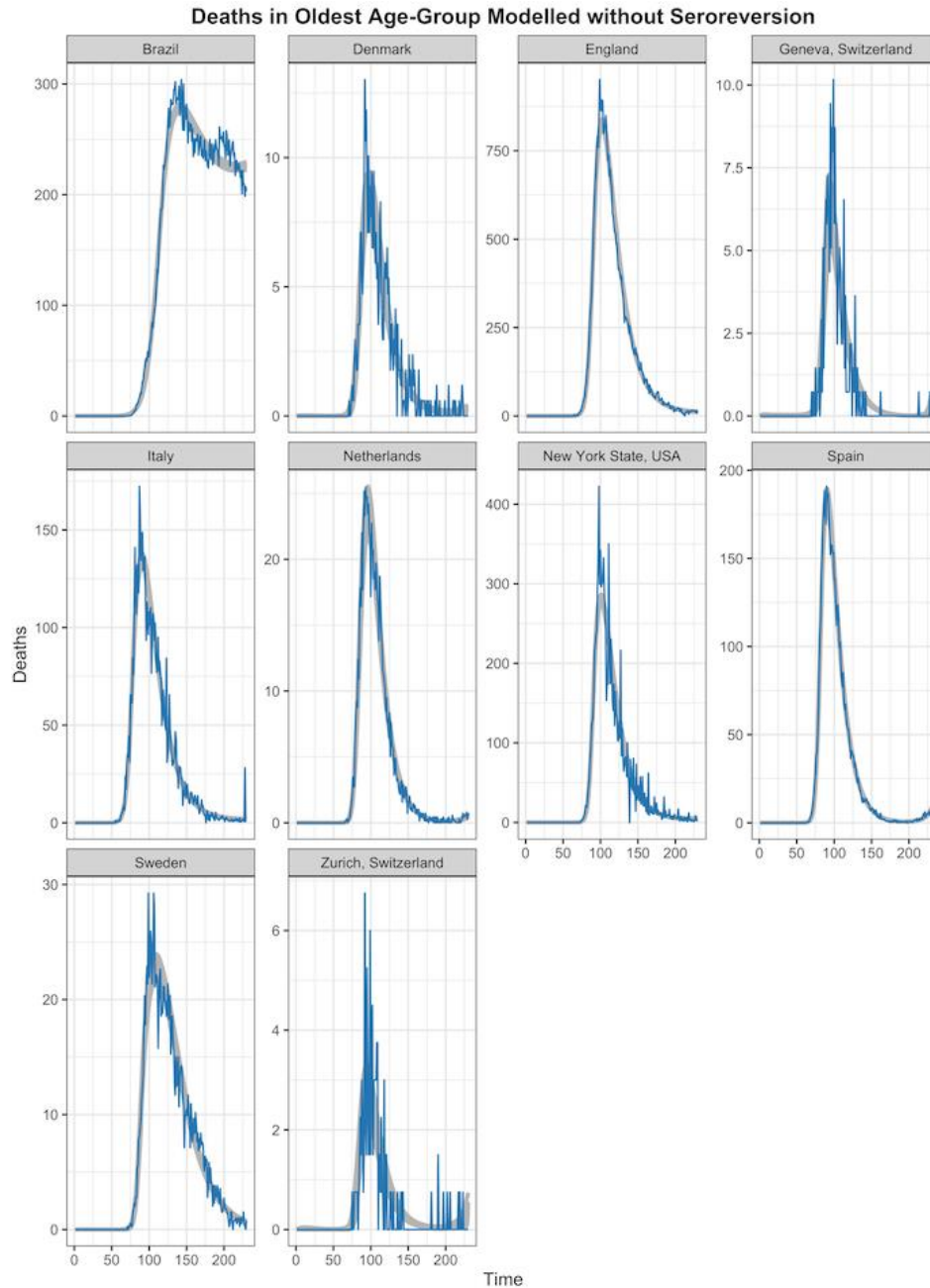
Sweden	(59,69]	2020-10-06	7.1	5.61 (5.27, 5.92)	5.42 (5.11, 5.89)	0.44 (0.3, 0.65)	0.67 (0.54, 0.91)	0.65 (0.52, 0.89)
Sweden	(69,79]	2020-10-06	7.1	5.56 (5.18, 6.04)	5.45 (5.09, 5.96)	1.53 (1.05, 2.25)	2.36 (1.94, 3.17)	2.26 (1.87, 3.13)
Sweden	(79,89]	2020-10-06	7.1	5.57 (5.07, 5.91)	5.47 (5.13, 5.83)	6.22 (4.33, 8.94)	10.05 (8.34, 13.51)	9.69 (8.01, 13.3)
Sweden	(89,999]	2020-10-06	7.1	5.54 (5.2, 5.98)	5.42 (5.05, 5.8)	15.22 (10.93, 20.98)	27.28 (22.61, 36.67)	26.18 (21.55, 35.99)
Geneva, Switzerland	(0,9]	2020-07-05	0	9.09 (8.31, 10.09)	9.04 (8.31, 9.85)		0 (0, 0.01)	0 (0, 0.01)
Geneva, Switzerland	(9,19]	2020-07-05	14.77	9.5 (8.54, 10.33)	9.45 (8.49, 10.31)	0 (0, 0)	0 (0, 0.01)	0 (0, 0.01)
Geneva, Switzerland	(19,29]	2020-07-05	11.41	9.77 (9.13, 10.44)	9.69 (9.08, 10.35)	0 (0, 0)	0 (0, 0.01)	0 (0, 0.01)
Geneva, Switzerland	(29,39]	2020-07-05	11.41	9.73 (8.86, 10.53)	9.67 (8.99, 10.44)	0.02 (0.02, 0.03)	0.02 (0, 0.06)	0.02 (0, 0.06)
Geneva, Switzerland	(39,49]	2020-07-05	11.41	9.69 (8.94, 10.64)	9.68 (8.9, 10.41)	0 (0, 0)	0 (0, 0.01)	0 (0, 0.01)
Geneva, Switzerland	(49,59]	2020-07-05	11.49	9.14 (8.39, 10.16)	9.19 (8.45, 10.31)	0.11 (0.08, 0.16)	0.12 (0.05, 0.21)	0.11 (0.05, 0.2)
Geneva, Switzerland	(59,69]	2020-07-05	11.49	9.1 (8.32, 10.06)	9.11 (8.44, 10.01)	0.26 (0.19, 0.39)	0.28 (0.15, 0.45)	0.27 (0.14, 0.44)
Geneva, Switzerland	(69,79]	2020-07-05	7.34	8.99 (8.02, 9.77)	8.91 (8.26, 9.76)	1.75 (1.01, 4.53)	1.28 (0.91, 1.74)	1.24 (0.88, 1.69)
Geneva, Switzerland	(79,999]	2020-07-05	7.34	8.84 (8.09, 9.71)	8.8 (7.98, 9.7)	9.33 (5.55, 21.53)	7.42 (6.03, 9.26)	7.18 (5.82, 8.96)
Zurich, Switzerland	(0,9]	16/05/2020	1.59	1.54 (1.38, 1.68)	1.55 (1.39, 1.72)	0 (0, 0)	0.01 (0, 0.02)	0.01 (0, 0.02)
Zurich, Switzerland	(9,19]	16/05/2020	1.59	1.54 (1.4, 1.71)	1.55 (1.37, 1.7)	0 (0, 0)	0.01 (0, 0.02)	0.01 (0, 0.02)
Zurich, Switzerland	(19,29]	16/05/2020	1.59	1.54 (1.38, 1.68)	1.54 (1.38, 1.68)	0 (0, 0)	0.01 (0, 0.02)	0.01 (0, 0.02)
Zurich, Switzerland	(29,39]	16/05/2020	1.59	1.54 (1.4, 1.69)	1.54 (1.39, 1.69)	0 (0, 0)	0.01 (0, 0.01)	0.01 (0, 0.01)
Zurich, Switzerland	(39,49]	16/05/2020	1.59	1.54 (1.41, 1.69)	1.53 (1.38, 1.69)	0 (0, 0)	0.01 (0, 0.01)	0.01 (0, 0.01)
Zurich, Switzerland	(49,59]	16/05/2020	1.59	1.52 (1.42, 1.66)	1.54 (1.38, 1.7)	0.12 (0.08, 0.18)	0.11 (0.02, 0.24)	0.11 (0.02, 0.24)

Zurich, Switzerland	(59,69]	16/05/2020	1.59	1.54 (1.42, 1.69)	1.55 (1.38, 1.71)	0.42 (0.3, 0.64)	0.42 (0.19, 0.73)	0.4 (0.18, 0.69)
Zurich, Switzerland	(69,79]	16/05/2020	1.59	1.54 (1.4, 1.67)	1.54 (1.41, 1.72)	0.91 (0.66, 1.39)	0.93 (0.52, 1.45)	0.89 (0.5, 1.39)
Zurich, Switzerland	(79,999]	16/05/2020	1.59	1.52 (1.36, 1.72)	1.54 (1.35, 1.66)	7.35 (5.42, 10.82)	8.01 (6.03, 10.53)	7.68 (5.82, 10.16)
New York State, USA	(0,9]	23/04/2020	12.49	12.26 (11.95, 12.71)	12.25 (11.81, 12.69)	0 (0, 0)	0 (0, 0)	0 (0, 0)
New York State, USA	(9,19]	23/04/2020	12.49	12.26 (11.81, 12.62)	12.27 (11.87, 12.71)	0 (0, 0)	0 (0, 0)	0 (0, 0)
New York State, USA	(19,29]	23/04/2020	12.49	12.27 (11.76, 12.73)	12.26 (11.86, 12.74)	0.02 (0.02, 0.02)	0.02 (0.02, 0.02)	0.02 (0.02, 0.02)
New York State, USA	(29,39]	23/04/2020	12.49	12.24 (11.89, 12.7)	12.27 (11.89, 12.7)	0.07 (0.07, 0.07)	0.07 (0.06, 0.08)	0.07 (0.06, 0.08)
New York State, USA	(39,49]	23/04/2020	12.49	12.25 (11.86, 12.75)	12.34 (11.86, 12.73)	0.2 (0.19, 0.22)	0.21 (0.19, 0.23)	0.2 (0.18, 0.23)
New York State, USA	(49,59]	23/04/2020	12.49	12.26 (11.88, 12.69)	12.3 (11.85, 12.7)	0.51 (0.48, 0.54)	0.53 (0.48, 0.58)	0.51 (0.47, 0.56)
New York State, USA	(59,69]	23/04/2020	10.89	11.12 (10.62, 11.61)	11.22 (10.79, 11.7)	1.4 (1.3, 1.5)	1.41 (1.29, 1.56)	1.37 (1.25, 1.51)
New York State, USA	(69,79]	23/04/2020	10.89	11.2 (10.71, 11.84)	11.26 (10.65, 11.69)	3.05 (2.85, 3.28)	3.13 (2.85, 3.46)	3.04 (2.77, 3.35)
New York State, USA	(79,999]	23/04/2020	10.89	11.18 (10.74, 11.68)	11.15 (10.65, 11.72)	7.2 (6.74, 7.71)	7.73 (7.05, 8.53)	7.51 (6.84, 8.25)

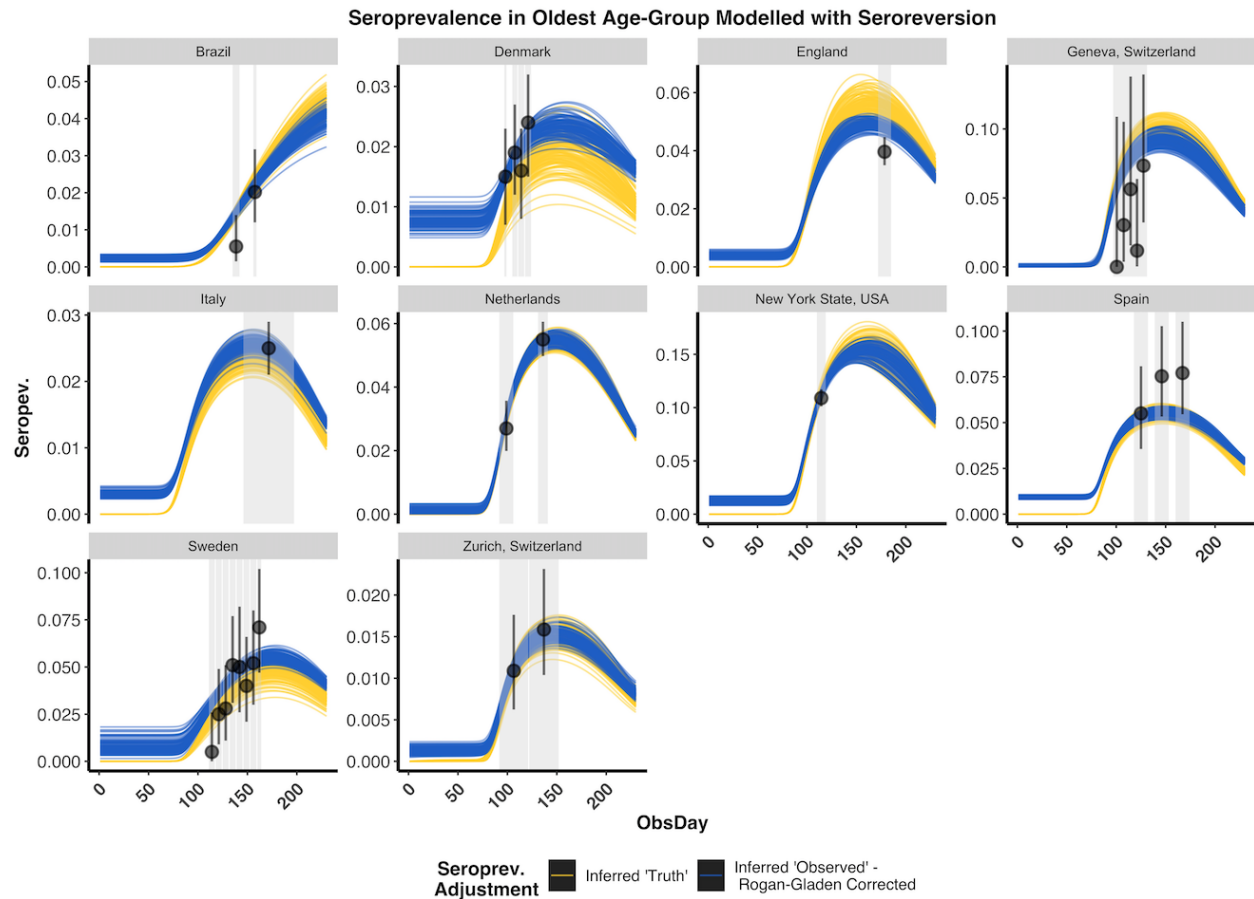
5.2 Posterior Predictive Checks



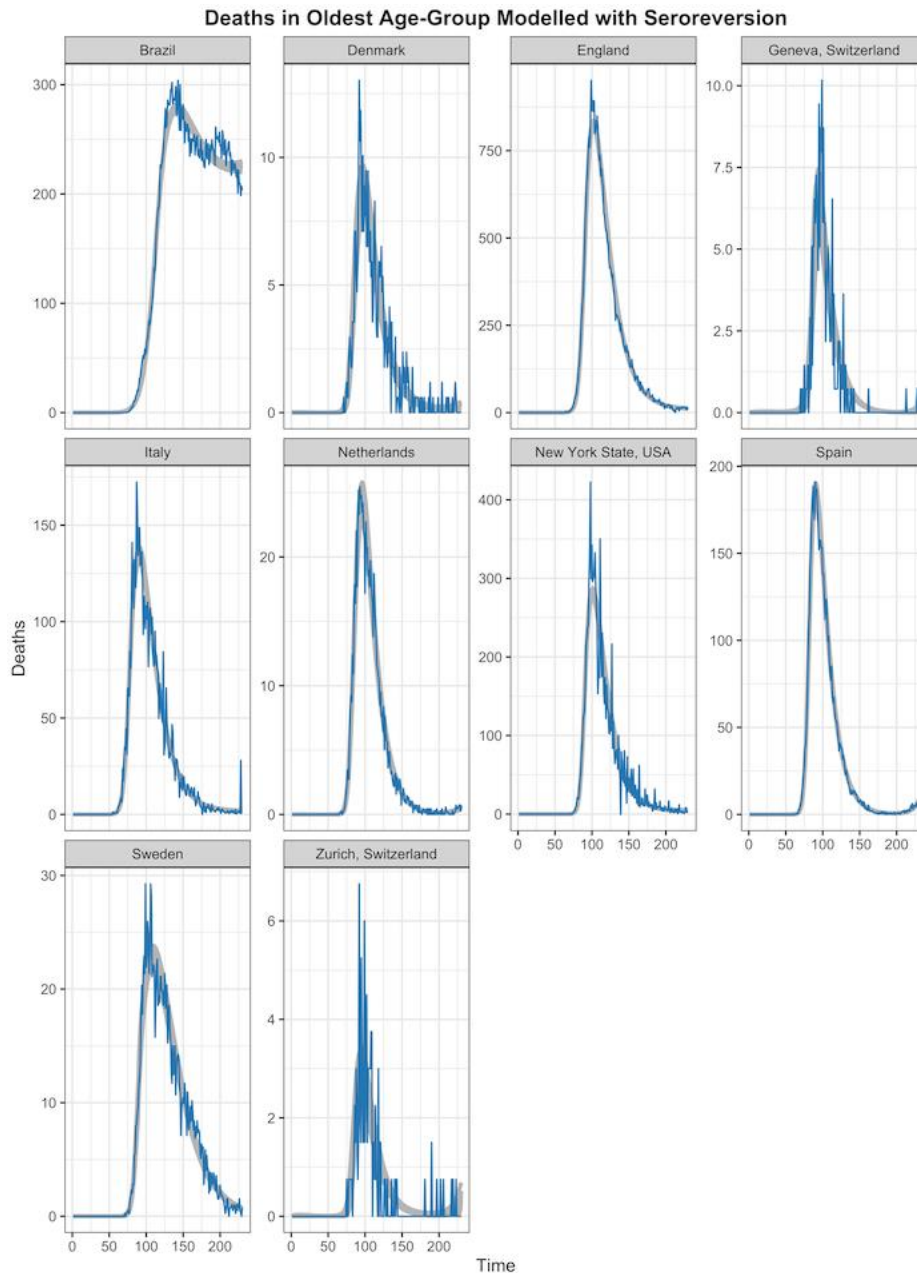
Supplementary Figure 6 - Posterior Draws of Modelled Seroprevalence without Seroreversion for the Oldest Age-Group: Results are presented from the statistical modelling framework where seroreversion was not included. For each study and its associated model fits, we selected 100 posterior draws of the modelled true seroprevalence (yellow) based on their posterior probabilities. Due to space constraints, we only show here the results for the oldest age group, although younger age-groups showed similar results. Given this true inferred seroprevalence, the expected observed seroprevalence, with the Rogan-Gladen correction, is also displayed (blue). The observed seroprevalence for the oldest age group is indicated along with its 95% confidence interval are indicated in black with the serostudy time-period demarcated by a grey box. The 95% confidence intervals were calculated using a binomial proportion with the exception of the Denmark, Italy, and Sweden studies, where reported seroprevalences and confidence intervals are plotted (binomial counts were not available). Overall, observed seroprevalences matched closely with modelled seroprevalence and varied in some instances due to the modelled differences in the distributions of infections across age-groups (Supplementary Table 6).



Supplementary Figure 7 - Posterior Predictive Check: Inferred Deaths without Seroreversion for the Oldest Age-Group: Results are presented from the statistical modelling framework where seroreversion was not included. For each study and its associated model fits we selected 100 posterior draws of the modelled IFR and delay of infection onset to death based on the posterior probabilities (grey). Inferred deaths were projected forward in time according to the gamma distribution fit and compared to the age-specific time-series deaths (*i.e.* model input: blue). Due to space constraints, we only show here the results for the oldest age group, although younger age-groups showed similar results.



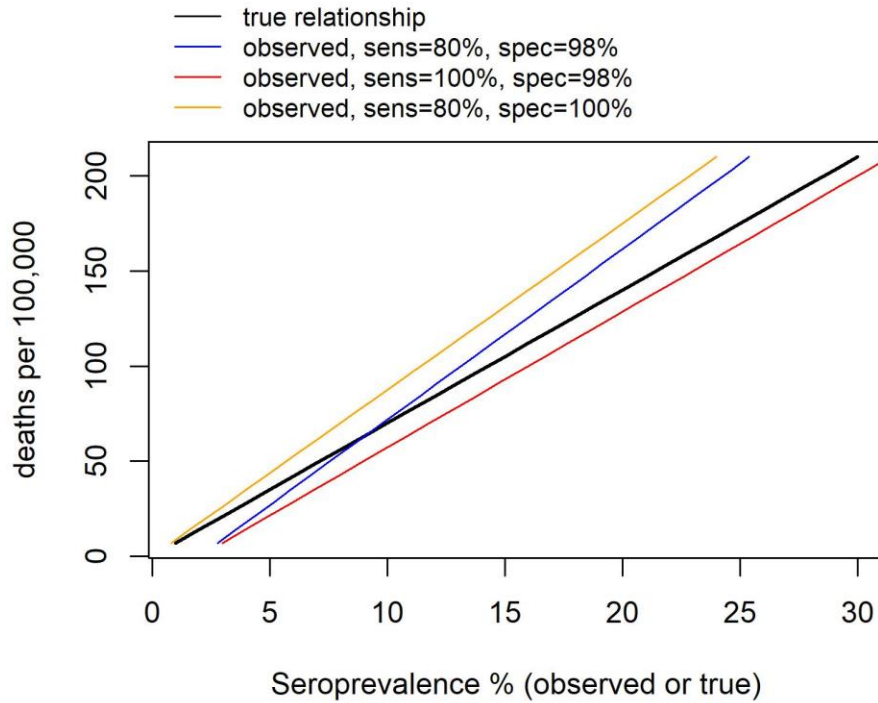
Supplementary Figure 8 - Posterior Draws of Modelled Seroprevalence with Seroreversion for the Oldest Age-Group: Results are presented from the statistical modelling framework where seroreversion was explicitly included. The seroreversion sensitivity analysis was used to present a conservative estimate of the IFR, as we assumed a fast rate of antibody waning from the Abbott assay (Muecksch *et al.* 2020). For each study and its associated model fits we selected 100 posterior draws of the modelled true seroprevalence (yellow) according to the posterior probabilities. Due to space constraints, we only show here the results for the oldest age group, although younger age-groups showed similar results. The rate of seroreversion after seroconversion was estimated from previously published data on the Abbott SARS-CoV-2 IgG assay, which demonstrated the greatest decay of sensitivity over time among the four assays evaluated (Muecksch *et al.* 2020). Given the true inferred seroprevalence, the expected observed seroprevalence, with the Rogan-Gladen correction, is also displayed (blue). Overall, observed seroprevalences matched closely with modelled seroprevalence and varied in some instances due to the modelled differences in the distributions of infections across age-groups (Supplementary Table 6). The effect of seroreversion later in the pandemic is apparent, particularly in Italy.



Supplementary Figure 9 - Posterior Predictive Check: Inferred Deaths with Seroreversion for the Oldest Age-Group: Results are presented from the statistical modelling framework where seroreversion was explicitly included. The seroreversion sensitivity analysis was used to present a conservative estimate of the IFR, as we assumed a fast rate of antibody waning from the Abbott assay (Muecksch *et al.* 2020). For each study and its associated model fits, we selected 100 posterior draws of the modelled IFR and delay of infection onset to death based on the posterior probabilities (grey). Inferred deaths were projected forward in time according to the gamma distribution fit and compared to the recasted age-specific time-series deaths (*i.e.* model input: blue). Due to space constraints, we only show here the results for the oldest age group, although younger age-groups showed similar results. The rate of seroreversion after seroconversion was estimated from previously published data on the Abbott SARS-CoV-2 IgG assay, which demonstrated the greatest decay of sensitivity over time among the four assays evaluated (Muecksch *et al.* 2020).

6. Estimating Specificity: Region-based Statistical Model Posteriors

6.1 Posterior Parameter Estimates

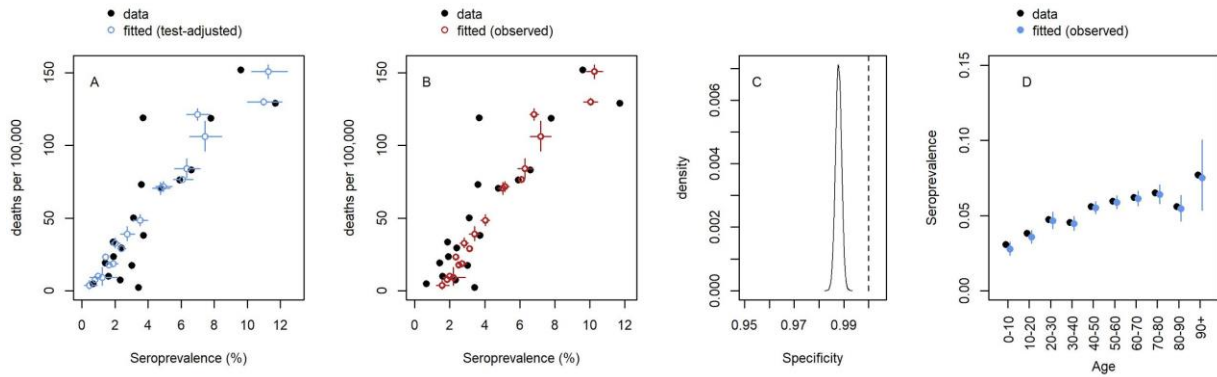


Supplementary Figure 10 - Expected relationship between seroprevalence and deaths per 100,000 under different values of serological test sensitivity and specificity, when overall IFR=0.7% and both IFR and population age structure are constant across all attack rates (seroprevalence values).

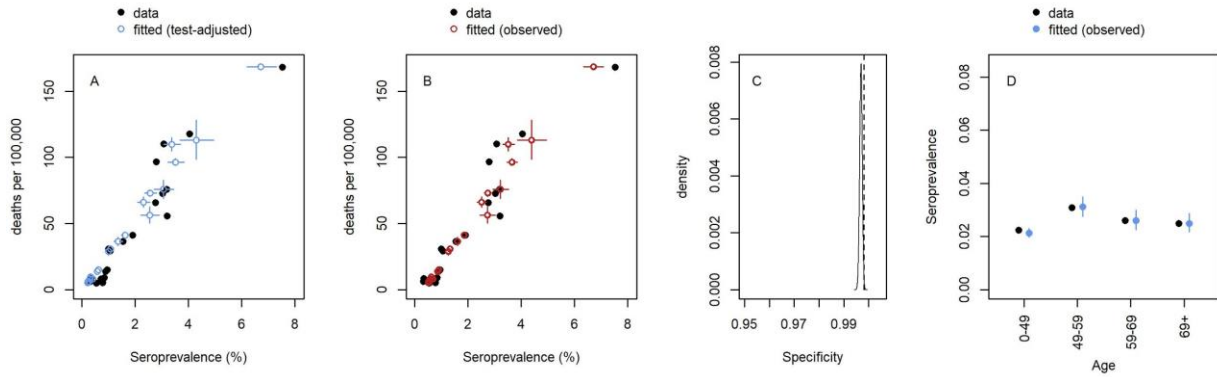
Supplementary Table 7 - Observed serovalidation results for each included studies and posterior estimates of sensitivity and specificity from regional and age-specific models: For each study, the number of test positives versus true positives reported were used to parameterize the sensitivity Beta-distributed prior in the age-specific IFR model. Similarly, the number of test negatives versus true negatives reported were used to parameterize the specificity Beta-distributed prior in the age-specific IFR model. For a subset of studies (6/10), regional information was used to re-estimate the true study sensitivity and specificity (using the region-based model). The resulting posterior medians and 95% credible intervals by study and model (without and with seroreversion) are provided for both the region-based and age-based model.

Study Location	Regional estimation of Sensitivity (95% CrI)	Re-estimation of Specificity (95% CrI)	Age-Specific Posterior Sensitivity without Seroreversion (95% CrI)	Age-Specific Posterior Specificity without Seroreversion (95% CrI)	Age-Specific Posterior Sensitivity with Seroreversion (95% CrI)	Age-Specific Posterior Sensitivity with Seroreversion (95% CrI)
Brazil	85.14 (81.93, 87.97)	99.72 (99.55, 99.85)	85.32 (82.12, 88.15)	99.76 (99.6, 99.86)	85.3 (82.11, 88.16)	99.76 (99.6, 99.86)
Denmark	82.09 (75.51, 87.58)	99.25 (98.94, 99.56)	82.46 (76.14, 87.77)	99.16 (98.72, 99.46)	82.4 (76.04, 87.7)	99.16 (98.72, 99.46)
England	78.4 (65.68, 88.15)	99.44 (99.11, 99.71)	79.89 (67.73, 89.43)	99.59 (99.34, 99.78)	80.05 (68.17, 89.24)	99.6 (99.34, 99.78)
Italy	96.04 (89.84, 99.05)	99.7 (99.59, 99.79)	96.52 (91.04, 99.13)	99.69 (99.57, 99.78)	96.53 (91.07, 99.18)	99.69 (99.57, 99.78)
Netherlands			98.22 (95.6, 99.5)	99.83 (99.45, 99.98)	98.24 (95.53, 99.52)	99.85 (99.46, 99.99)
Spain	81.84 (75.67, 87.01)	98.79 (98.55, 99.02)	84.73 (83.09, 88.44)	99.04 (98.85, 99.21)	84.74 (83.09, 88.46)	99.05 (98.86, 99.22)
Sweden			99.3 (97.22, 99.94)	99.16 (98.13, 99.76)	99.3 (97.21, 99.94)	99.14 (98.04, 99.75)
Geneva, Switzerland			91.44 (86.93, 94.87)	99.89 (98.73, 100)	91.45 (86.77, 94.84)	99.89 (98.75, 100)
Zurich, Switzerland			91.76 (83.18, 96.89)	99.87 (99.74, 99.95)	91.78 (83.49, 96.92)	99.87 (99.74, 99.95)
New York State, USA	89.39 (85.57, 92.55)	98.73 (98.15, 99.27)	89.69 (85.89, 92.72)	98.69 (98, 99.2)	89.68 (85.89, 92.82)	98.69 (98.03, 99.19)

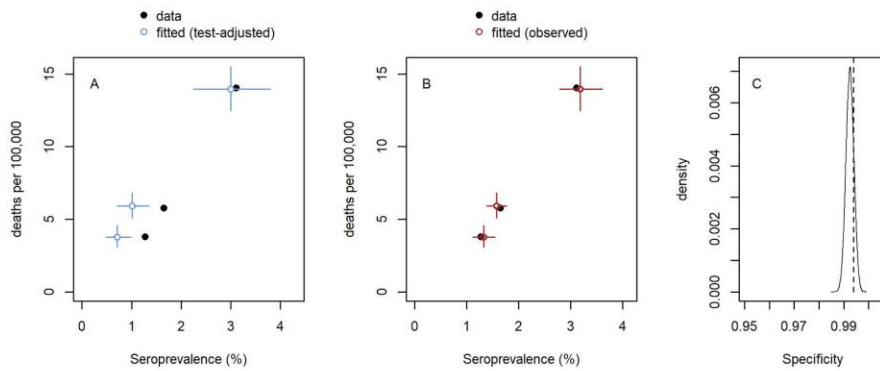
Spain



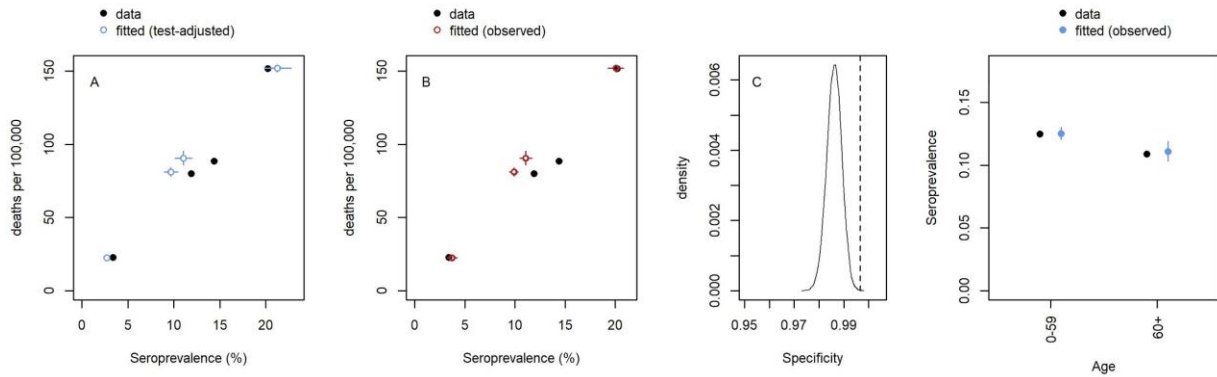
Italy



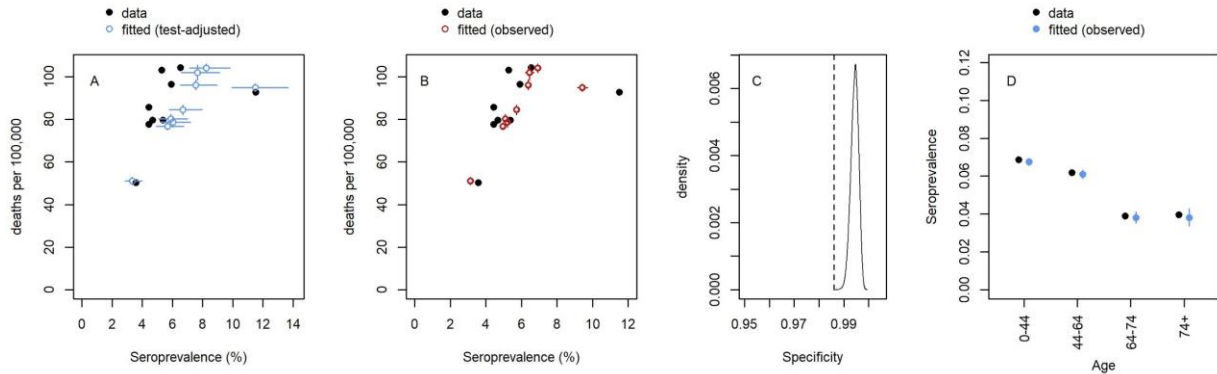
Denmark (average seroprevalence across all ages assumed to be the same due to lack of overlap of mortality and seroprevalence data age groups)



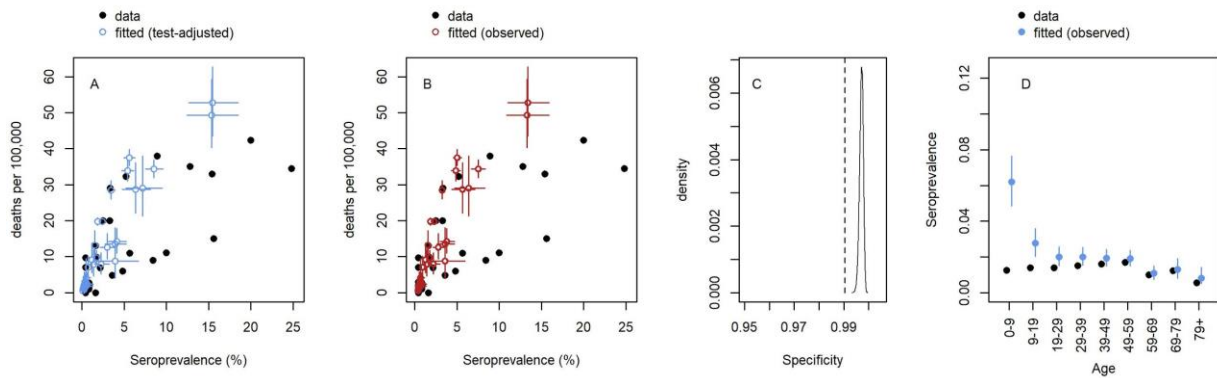
New York State



England



Brazil

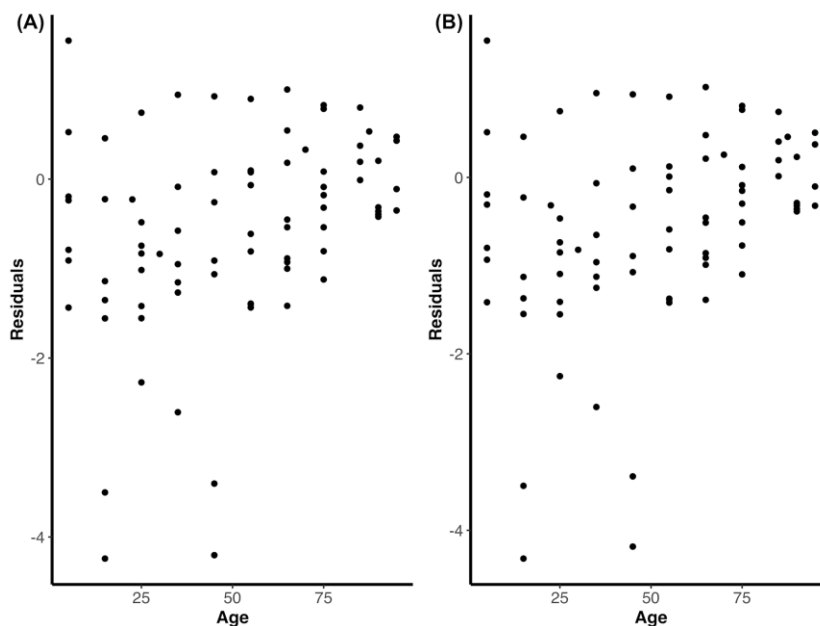


Supplementary Figure 11 - Regional model fits to data for six studies where serosurvey data and mortality could be broken down by region: For each country: (A) relationship between seroprevalence and COVID-19 mortality per 100,000 population in the data (observed seroprevalence not adjusted for test sensitivity and specificity) and model-estimated true seroprevalence (adjusted for test sensitivity and specificity) and mortality with 95% credible intervals. (B) as A but showing model-estimated observed seroprevalence (as would be observed given the model-estimated sensitivity and specificity). (C) Specificity posterior distribution (solid line) versus the value reported in the study (dashed line) (D) Observed versus model-estimated age-specific seroprevalence (as would be observed given the model-estimated sensitivity and specificity).

7. Pooled IFR Calculation

We pooled the posterior age-specific IFR estimates across studies using weighted log-linear regression, where weights were calculated as the posterior precision of age- and study-specific IFR estimates. After fitting the weighted log-linear regression model, we found that there was heteroskedasticity in the model residuals (**Supplementary Figure 12**). To account for this, we modelled variance as a quadratic equation with respect to the mean age within each age-group for each study categorized into one of the 10-year age bands (**Table 3**). Our final model therefore consists of a fitted linear model for the mean of the $\log(\text{IFR})$ by age, with the variance in $\log(\text{IFR})$ changing with age. Under the assumption of normally distributed residuals in log space, this corresponds to a log-normal model in linear space, in which the mean is a function of both the mean and the variance in $\log(\text{IFR})$. This log-normal model was used to produce the final predictive intervals in 5-year age bands.

We then standardized these age-specific estimates to the population demographics of four countries: Madagascar, Nicaragua, Grenada and Malta, which have previously been identified as representative countries for each of the World Bank Income Strata: LIC, LMIC, UMIC, and HIC (see **Data Extraction and Collation** section above)⁴. The overall IFR prediction interval was estimated using a Monte Carlo sampling approach: repeatedly drawing from the appropriate log-normal distribution (as described above) and combining values as weighted sums, where weights were calculated from the age-specific demographics.



Supplementary Figure 12 - Weight Log-Linear Model Residuals: The model residuals from the weighted log-linear pooled fits are shown when seroreversion was not considered (**A**) and was considered (**B**). The residuals show heteroscedasticity, particularly among the middle age-groups.

Supplementary Table 8 - Variance within the 10-year Age-Groups for the Pooled IFR estimates Log-Linear Model Residuals: The corresponding variance for the 10-year age-groups calculated from the modelled residuals and used in the pooled IFR calculations.

Age	Variance from Modelled Estimates without Seroreversion	Variance from Modelled Estimates with Seroreversion
5	0.9935	0.9916
15	2.8285	2.8956
25	0.7423	0.7289
35	1.0318	1.0319
45	3.4969	3.468
55	0.6755	0.6583
65	0.6404	0.6227
75	0.4056	0.3794
85	0.0967	0.0765
95	0.1335	0.1222

8. References

- 1 Arora RK, Joseph A, Van Wyk J, *et al.* SeroTracker: a global SARS-CoV-2 seroprevalence dashboard. *Lancet Infect Dis* 2020; published online Aug 4. DOI:10.1016/S1473-3099(20)30631-9.
- 2 Dong E, Du H, Gardner L. An interactive web-based dashboard to track COVID-19 in real time. *Lancet Infect Dis* 2020; **20**: 533–4.
- 3 COVID-19 Data Repository by the Center for Systems Science and Engineering (CSSE) at Johns Hopkins University. <https://github.com/CSSEGISandData/COVID-19>.
- 4 Walker PGT, Whittaker C, Watson OJ, *et al.* The impact of COVID-19 and strategies for mitigation and suppression in low- and middle-income countries. *Science* 2020; published online June 12. DOI:10.1126/science.abc0035.
- 5 United Nations, Department of Economic and Social Affairs Population Dynamics. World Population Prospects 2019. <https://population.un.org/wpp>.
- 6 Whitman JD, Hiatt J, Mowery CT, *et al.* Test performance evaluation of SARS-CoV-2 serological assays. *medRxiv* 2020; published online May 17. DOI:10.1101/2020.04.25.20074856.
- 7 Hallal PC, Hartwig FP, Horta BL, *et al.* SARS-CoV-2 antibody prevalence in Brazil: results from two successive nationwide serological household surveys. *Lancet Glob Health* 2020; **8**: e1390–8.
- 8 SRAG 2020 - Severe Acute Respiratory Syndrome Database - including data from COVID-19. <https://opendatasus.saude.gov.br/dataset/bd-srag-2020>.
- 9 Instituto Brasileiro Geografi. Projeções da População. <https://www.ibge.gov.br/estatisticas/sociais/populacao/9109-projecao-da-populacao.html?=&t=resultados>.
- 10 Erikstrup C, Hother CE, Pedersen OBV, *et al.* Estimation of SARS-CoV-2 infection fatality rate by real-time antibody screening of blood donors. *Clin Infect Dis* 2020; published online June 25. DOI:10.1093/cid/ciaa849.
- 11 Coronavirus: Som bloddonor hjælper du nu med at afdække det danske mørketal - Bloddonorerne i Danmark. <https://bloddonor.dk/coronavirus/> (accessed Sept 28, 2020).
- 12 Tal og overvågning: COVID-19. <https://www.sst.dk/da/corona/tal-og-overvaagning> (accessed Sept 28, 2020).
- 13 Statens Serum Institute, Denmark. Overvågning af COVID-19. <https://www.ssi.dk/sygdommeberedskab-og-forskning/sygdomsovervaagning/c/covid19-overvaagning>.
- 14 Statistik D. Statistikbanken. 2011. <https://www.statistikbanken.dk/statbank5a/>.
- 15 Comas-Herrera A, Zalakaín J, Litwin C, Hsu AT, Lane N, Fernández J-L. Mortality associated with COVID-19 outbreaks in care homes: early international evidence. *LTCcovid org, International Long-Term Care Policy Network* 2020. <https://ltccovid.org/2020/04/12/mortality-associated-with-covid-19-outbreaks-in-care-homes-early-international-evidence/>.

- 16 Flower B, Brown JC, Simmons B, *et al.* Clinical and laboratory evaluation of SARS-CoV-2 lateral flow assays for use in a national COVID-19 seroprevalence survey. *Thorax* 2020; published online Aug 12. DOI:10.1136/thoraxjnl-2020-215732.
- 17 Ward H, Atchison CJ, Whitaker M, *et al.* Antibody prevalence for SARS-CoV-2 in England following first peak of the pandemic: REACT2 study in 100,000 adults. *medRxiv* 2020; : 2020.08.12.20173690.
- 18 Excess mortality in England, week ending 17 July 2020. <https://fingertips.phe.org.uk/static-reports/mortality-surveillance/excess-mortality-in-england-week-ending-17-Jul-2020.html>.
- 19 Deaths registered weekly in England and Wales, provisional. <https://www.ons.gov.uk/peoplepopulationandcommunity/birthsdeathsandmarriages/deaths/datasets/weeklyprovisionalfiguresondeathsregisteredinenglandandwales>.
- 20 Population Estimates. <https://www.ons.gov.uk/peoplepopulationandcommunity/populationandmigration/populationestimates>.
- 21 Deaths involving COVID-19 in the care sector, England and Wales. <https://www.ons.gov.uk/peoplepopulationandcommunity/birthsdeathsandmarriages/deaths/datasets/deathsinvolvingcovid19inthecaresectorenglandandwales>.
- 22 Primi Risultati Dell'indagine Di Sieroprevalenza Sul SARS-CoV-2. <https://www.istat.it/it/files//2020/08/ReportPrimiRisultatiIndagineSiero.pdf>.
- 23 Ng DL, Goldgof GM, Shy BR, *et al.* SARS-CoV-2 seroprevalence and neutralizing activity in donor and patient blood from the San Francisco Bay Area. *medRxiv* 2020; published online May 25. DOI:10.1101/2020.05.19.20107482.
- 24 Italian Ministry of Health. <http://www.salute.gov.it/portale/nuovocoronavirus/>.
- 25 Resident population by age, sex and marital status and Resident Foreigners by age and sex. 2014; published online Sept 29. <https://www.istat.it/en/archivio/132669> (accessed Sept 28, 2020).
- 26 Slot E, Hogema BM, Reusken CB, *et al.* Herd immunity is not a realistic exit strategy during a COVID-19 outbreak. 2020.
- 27 Reuters Staff. Study shows coronavirus antibodies in 5.5% of Dutch blood donors. <https://uk.reuters.com/article/uk-health-coronavirus-netherlands-study/study-shows-coronavirus-antibodies-in-5-5-of-dutch-blood-donors-idUKKBN23A00T>.
- 28 Covid-19 karakteristieken per casus landelijk. <https://data.rivm.nl/geonetwork/srv/dut/>.
- 29 National Institute for Public Health and the Environment, Ministry of Health, Welfare and Sport, the Netherlands. Development of COVID-19 in Graphs. <https://www.rivm.nl/coronavirus-covid-19/grafieken>.
- 30 CBS Dataportaal. <https://opendata.cbs.nl/statline/portal.html> (accessed Sept 28, 2020).
- 31 Pollán M, Pérez-Gómez B, Pastor-Barriuso R, *et al.* Prevalence of SARS-CoV-2 in Spain (ENE-COVID):

- a nationwide, population-based seroepidemiological study. *Lancet* 2020; **396**: 535–44.
- 32 Ministerio de Sanidad, Consumo y Bienestar Social - Ciudadanos - Estudio Nacional de sero-Epidemiología de la Infección por SARS-CoV-2 en España (ENE-Covid). <https://www.msbs.gob.es/ciudadanos/ene-covid/> (accessed Sept 28, 2020).
 - 33 Spanish Ministry of Health (Data obtained from the database The demography of deaths by COVID-19). National Institute of Demographic Studies (INED) (distributor). Extracted from: <https://dc-covid.site.ined.fr/fr/> (16/10/20).
 - 34 INE. Instituto Nacional de Estadística. <https://www.ine.es/> (accessed Sept 28, 2020).
 - 35 Sweden Public Health Agency. Påvisning av antikroppar efter genomgången covid-19 i blodprov från öppenvården (Delrapport 1). <https://www.folkhalsomyndigheten.se/contentassets/9c5893f84bd049e691562b9eeb0ca280/pavisning-antikroppar-genomgangen-covid-19-blodprov-oppenvarden-delrapport-1.pdf>.
 - 36 Sweden Public Health Agency. Påvisning av antikroppar efter genomgången covid-19 hos blodgivare (Delrapport 2). <https://www.folkhalsomyndigheten.se/contentassets/376f9021a4c84da08de18ac597284f0c/pavisning-antikroppar-genomgangen-covid-19-blodgivare-delrapport-2.pdf>.
 - 37 Sweden Public Health Agency. Bekräftade fall i Sverige – daglig uppdatering. <https://www.folkhalsomyndigheten.se/smittydd-beredskap/utbrott/aktuella-utbrott/covid-19/bekraftade-fall-i-sverige/>.
 - 38 Folkhalsomyndigheten Public Health Agency of Sweden. Bekräftade fall i Sverige – daglig uppdatering. <https://www.folkhalsomyndigheten.se/smittydd-beredskap/utbrott/aktuella-utbrott/covid-19/statistik-och-analyser/bekraftade-fall-i-sverige/>.
 - 39 Folkmängden efter region, civilstånd, ålder och kön. År 1968 - 2019. http://www.statistikdatabasen.scb.se/pxweb/sv/ssd/START_BE_BE0101_BE0101A/BefolkningNy/?rxid=938858cd-aeaf-4a53-80de-7b060f869878.
 - 40 Meyer B, Torriani G, Yerly S, *et al.* Validation of a commercially available SARS-CoV-2 serological immunoassay. *Clin Microbiol Infect* 2020; **26**: 1386–94.
 - 41 Stringhini S, Wisniak A, Piumatti G, *et al.* Seroprevalence of anti-SARS-CoV-2 IgG antibodies in Geneva, Switzerland (SEROCoV-POP): a population-based study. *Lancet* 2020; **396**: 313–9.
 - 42 Federal Office of Public Health. COVID-19 en Suisse. <https://covid-19-schweiz.bagapps.ch/fr-1.html>.
 - 43 Federal Office of Public Health. Situation in Switzerland. <https://www.bag.admin.ch/bag/en/home/krankheiten/ausbrueche-epidemien-pandemien/aktuelle-ausbrueche-epidemien/novel-cov/situation-schweiz-und-international.html>.
 - 44 Mehr als die Hälfte starb in Alters- und Pflegeheimen. <https://interaktiv.tagesanzeiger.ch/2020/corona-tote-mehrheitlich-aus-altersheimen/>.
 - 45 Emmenegger M, De Cecco E, Lamparter D, *et al.* Early plateau of SARS-CoV-2 seroprevalence

- identified by tripartite immunoassay in a large population. *medRxiv* 2020. <https://www.medrxiv.org/content/10.1101/2020.05.31.20118554v2.full>.
- 46 Rosenberg ES, Tesoriero JM, Rosenthal EM, *et al.* Cumulative incidence and diagnosis of SARS-CoV-2 infection in New York. *Ann Epidemiol* 2020; **48**: 23–9.e4.
 - 47 New York State Department of Health. Fatalities. <https://covid19tracker.health.ny.gov/views/NYS-COVID19-Tracker/NYSDOHCOVID-19Tracker-Fatalities>.
 - 48 United States Census Bureau. County Population by Characteristics: 2010-2019. <https://www.census.gov/data/tables/time-series/demo/popest/2010s-counties-detail.html>.
 - 49 State Data and Policy Actions to Address Coronavirus. <https://www.kff.org/health-costs/issue-brief/state-data-and-policy-actions-to-address-coronavirus/#stateleveldata>.
 - 50 Muecksch F, Wise H, Batchelor B, *et al.* Longitudinal analysis of clinical serology assay performance and neutralising antibody levels in COVID19 convalescents. *medRxiv* 2020; published online Aug 6. DOI:10.1101/2020.08.05.20169128.
 - 51 Therneau TM, Grambsch PM. Modeling Survival Data: Extending the Cox Model. Springer Science & Business Media, 2000.
 - 52 Therneau TM. A Package for Survival Analysis in R. 2020 <https://CRAN.R-project.org/package=survival>.
 - 53 Kassambara A, Kosinski M, Biecek P. survminer: Drawing Survival Curves using ‘ggplot2’. 2020. <http://www.sthda.com/english/rpkgs/survminer/>.
 - 54 Borremans B, Gamble A, Prager KC, *et al.* Quantifying antibody kinetics and RNA shedding during early-phase SARS-CoV-2 infection. *medRxiv* 2020. <https://www.medrxiv.org/content/10.1101/2020.05.15.20103275v1.abstract>.
 - 55 Li Q, Guan X, Wu P, *et al.* Early Transmission Dynamics in Wuhan, China, of Novel Coronavirus–Infected Pneumonia. *N Engl J Med* 2020; **382**: 1199–207.
 - 56 Linton NM, Kobayashi T, Yang Y, *et al.* Incubation Period and Other Epidemiological Characteristics of 2019 Novel Coronavirus Infections with Right Truncation: A Statistical Analysis of Publicly Available Case Data. *J Clin Med Res* 2020; **9**. DOI:10.3390/jcm9020538.
 - 57 Delignette-Muller ML, Dutang C. fitdistrplus: An R Package for Fitting Distributions. *Journal of Statistical Software*. 2015; **64**: 1–34.
 - 58 Verity R, Okell LC, Dorigatti I, *et al.* Estimates of the severity of coronavirus disease 2019: a model-based analysis. *Lancet Infect Dis* 2020; published online March 30. DOI:10.1016/S1473-3099(20)30243-7.
 - 59 Wood SN, Wit EC, Fasiolo M, Green PJ. COVID-19 and the difficulty of inferring epidemiological parameters from clinical data. *Lancet Infect Dis* 2020; published online May 28. DOI:10.1016/S1473-3099(20)30437-0.

- 60 Salje H, Tran Kiem C, Lefrancq N, *et al.* Estimating the burden of SARS-CoV-2 in France. *Science* 2020; **369**: 208–11.
- 61 Verity R, Winskill P. drjacoby: Flexible Markov Chain Monte Carlo via Reparameterization. <https://github.com/mrc-ide/drjacoby>.
- 62 Gelman A, Rubin DB. Inference from Iterative Simulation Using Multiple Sequences. *Stat Sci* 1992; **7**: 457–72.
- 63 Carpenter B, Gelman A, Hoffman MD, *et al.* Stan: A probabilistic programming language. *J Stat Softw* 2017; **76**. <https://www.osti.gov/biblio/1430202>.
- 64 Rogan WJ, Gladen B. Estimating prevalence from the results of a screening test. *Am J Epidemiol* 1978; **107**: 71–6.